The International Journal of Advanced Manufacturing Technology (2018) 97:3999–4019
https://doi.org/10.1007/s00170-018-2019-5

ORIGINAL ARTICLE

Synthesis and recent advances in tribological applications of graphene

Ashish K. Kasar[1] · Pradeep L. Menezes[1]

Received: 6 January 2018 / Accepted: 4 April 2018 / Published online: 5 June 2018

Abstract
Graphene is one of the most emerging material in the field of nanotechnology, and it is gaining a tremendous amount of research interest in recent years. Apart from its unique electronic, electrical, mechanical, and thermal properties, graphene also possesses lower wear rate and friction coefficient. The superior tribological properties of graphene have attracted many researchers to synthesize self-lubricating nanocomposite materials that can have several applications in the automobile, aerospace, and marine industries. Graphene is also proven a competitive nanomaterial as an additive in the lubricant oil because of stable suspension and improved anti-wear properties of the component. This article aims to present the review of the advancement in the field of graphene synthesis; tribological properties of graphene; the role of graphene as reinforcement in polymer-matrix, metal-matrix, and ceramic-matrix nanocomposites; and also graphene as an additive in lubricant oil. The results reveal that addition of graphene to the composites can lead to decrease both wear rate and coefficient of friction for all three class of materials. Moreover, when graphene used as a lubricant additive, it improves the load carrying capacity of lubricant oil along with decreased friction and wear. Performance of graphene-reinforced composites and graphene suspended lubricants depend on various tribological and materials parameters which are discussed in this article. The limitation of present knowledge and future research scope are also highlighted.

Keywords Graphene · Tribology · Polymer-matrix composites · Metal-matrix composites · Ceramic-matrix composites

1 Introduction

Graphene is a two-dimensional hexagonal structure of carbon atoms. In recent years, it has gained tremendous amount of attention due to its extraordinary properties such as physical, mechanical, and thermal [1–3]. These properties of graphene are compared with common structure steel ASTM A36 and copper in Table 1. It can be seen that graphene is 200 to 300 times stronger than the ASTM A36 steel and it has seven times higher thermal conductivity than the copper.

One of the most promising application of graphene is as lubricant material. Graphene has found to have the best tribological properties. The most common parameters to characterize the tribological properties are coefficient of friction (COF) and wear rate. The COF is the ratio of frictional force to normal force when two bodies are in contact and moving relative to each other, whereas the wear rate ($m^3\ m^{-1}$) is volume loss per unit distance. Often, wear is defined by specific wear rate ($m^3\ N^{-1}\ m^{-1}$) which depends on the applied load to cause wear. Several researchers investigated the tribological properties of graphene. Berman et al. [8] demonstrated that the single-layer graphene-coated steel substrate stays for 6500 cycles in the tribological test using a steel ball whereas other materials, such as MoS_2 and diamond-like carbon, stay maximum up to 1000 cycles. Graphene reinforcement also provides lower component weight due to its lower density [4]. The tribological properties of graphene along with the other properties, such as mechanical and thermal, can be utilized by formation of self-lubricated composite materials. Composite material consists of two or more different materials and provides superior properties than the constituent materials. A comparative data is plotted in Fig. 1 for epoxy polymer [9], TiAl alloy [10], and Si_3N_4 ceramic-matrix composites [11]. It can be seen that by addition of graphene, COF goes down for all the three materials named as epoxy + 2.5 wt.% graphene, TiAl alloy + 3.5 wt.% graphene, and Si_3N_4 + 3 wt.% graphene. It suggests that graphene can significantly improve

✉ Pradeep L. Menezes
pmenezes@unr.edu

[1] Department of Mechanical Engineering, University of Nevada Reno, Reno, NV 89557, USA

Table 1 Physical, mechanical, and thermal properties comparison of graphene with Cu and Steel ASTM36

Material	Density (gm/cm^3)	Tensile strength (MPa)	Young's modulus (GPa)	Thermal conductivity (W/(m-K))
Graphene	1.5–2.0 [4]	130×10^3 [1]	1×10^3 [1]	~3080–5150 [3]
Cu annealed	8.9 [5]	210 [5]	110 [5]	398 [5]
Steel, ASTM A36	7.8 [6]	400–550 [6]	200 [6]	50 [7]

the tribological properties of graphene-based composites in all three classes of materials that are polymer, metal, and ceramic.

The current focus of the study about the tribology of graphene is to utilize graphene in the composite for the development of self-lubricating composites and for the lubricating oils as an additive for the development of multiphase lubricating fluids to enhance tribological performance. Properties of graphene-reinforced composites also rely on the graphene synthesis techniques because different techniques have their pros and cons, such as number of graphene layers, size, and defects. Apart from the traditional techniques (chemical vapor deposition, chemical route by graphene oxide), other novel techniques, for example ball milling, electrochemical exfoliation, have also been explored. In this paper, we are reviewing the various synthesis process for graphene, tribological properties of graphene, graphene-reinforced self-lubricating nanocomposites and application of graphene as an additive in lubricant oil.

2 Synthesis of graphene

Synthesis of high-quality graphene remains a challenge; different methods have their own drawbacks. Understanding of graphene synthesis is highly important. Peng et al. [12] studied the effect of different graphene synthesis techniques on tribological properties. The authors reported high lubrication and zero wear on defect-free graphene nanosheets produced by mechanical exfoliation, whereas the chemical vapor deposition-grown graphene and reduced graphene oxide graphene have poor tribological properties due to destroyed graphitic structure. Apart from defects, other factors such as size, surface area, number of layers, chemical inertness, and mechanical properties are determining factors. Desired quality and form of graphene vary according to the application. Knowledge of required properties as per the application and understanding of graphene synthesis techniques can help the researcher to achieve goals in individual research.

Graphene synthesis techniques can be divided into two categories: top-down and bottom-up techniques. As the name suggests, in top-down technique, the graphene is synthesized by separating the layers from a graphitic structure, such as exfoliation and cleavage method, whereas in bottom-up technique, graphene is formed by deposition of carbon atoms on a substrate as in chemical vapor deposition techniques. Various processing routes for graphene synthesis are described below.

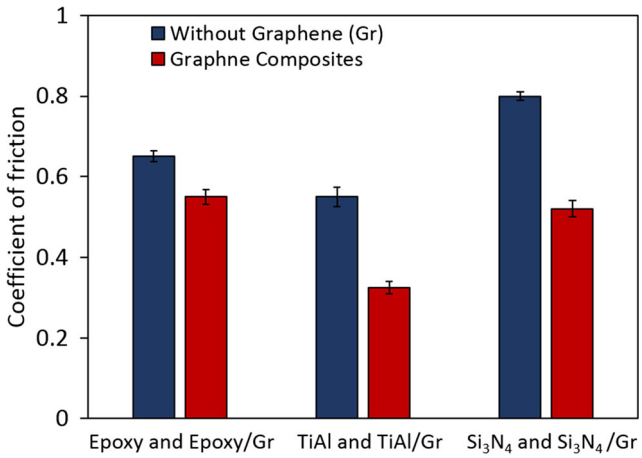

Fig. 1 Reduction in coefficient of friction by addition of graphene (Gr) in epoxy [9], TiAl alloy [10], and Si_3N_4 matrix [11]

2.1 Exfoliation and cleavage

This method involves the separation of carbon layers from the graphitic structure by breaking the covalent bond between interlayer carbon atoms. For the first time in 2003, Viculis et al. [13] produced the graphitic layers by exfoliation. In this work, the authors used a potassium compound (KC_8) to intercalate the high-purity graphite. The exothermic reaction between KC_8 and aqueous solution caused the separation of graphitic layers. After sonication for 1 h, it resulted in scrolling up and formed nanoscrolls. TEM studies confirmed that each nanoscroll consisted of 40 ± 15 layers. Although the produced graphene was thicker but this study indicated that exfoliation could be one of the possible ways to synthesize graphene layers.

In 2004, Novoselov et al. [14] successfully produced the graphene by exfoliation process. They created many ~5 μm deep mesas by dry etching the highly oriented pyrolytic graphite in the oxygen plasma. Then these mesas were stuck to the photoresist followed by peeling off the layers by scotch tape. The rest thin attached layers on photoresist were discharged in acetone and then transferred to Si substrate, which resulted in the deposition of single- and few-layer graphene. This simple method turns out to be reliable and later it used to synthesize graphene for several studies [15–17].

Huc et al. [18] improved the scotch tape technique to produce larger graphene sheets. In place of scotch tape, the authors used a substrate and epoxy glue to bond the substrate and graphene source (highly oriented pyrolytic graphite). This method formed a larger (~ 10 μm) and flatted few sheets of graphene. This approach was further modified by using an insulating substrate having ionic conductivity [19]. Anodic bonding was developed between graphite and substrate material by applying voltage. The achieved bonding was cleaved off and left graphene layers on the substrate which were peeled off by adhesive tape and resulted in one or few-layer graphene.

Exfoliation of graphite carried out several other ways as well. Zhao et al. [20] produced the graphene using wet ball milling techniques. In this work, the authors first dispersed the 0.02 g of graphite nanosheets in 80 mL of anhydrous N,N-dimethylformamide followed by milling for 30 h with zirconia balls. Due to shear force, graphitic layer got exfoliated and resulted in the dark homogeneous colloidal suspension of graphene. After evaporation of liquid media, single- and few-layer graphene were obtained. Lie et al. [21] showed that exfoliation could also be achieved by expansion of graphitic structure which leads to graphene formation. In this work, the authors first dispersed the expandable graphite in N,N-dimethylformamide and then heated in stainless steel reactor for 15 min at 377 °C. Due to thermal expansion exfoliation occurred. The produced graphene layers were vacuum dried and obtained in powder form.

Graphene nanosheets can also be synthesized by electrochemical exfoliation of graphite. Liu et al. [22] have shown that functionalized graphene nanosheets can be produced by ionic liquid treated graphite. The authors used different ionic liquids such as 1-octyl-3-methyl-imidazolium hexafluorophosphate in water and applied 10 to 20 V between two graphite electrodes. After 6 h of corrosion, the functional graphene sheets were extracted from the electrolyte. The electrochemical exfoliation method has been adopted in various studies. In one of the study, Wang et al. [23] produced graphene layers from a negative graphite electrode in the electrolyte of Li^+/propylene carbonate under a potential of 15 ± 5 V. The obtained graphene layers were thick up to 5 layers. Higher lateral sized graphene layer up to 30 μm has also been synthesized by electrochemical exfoliation [24]. It was obtained by electrochemical exfoliation of highly oriented pyrolytic graphite anode in the solution of 4.8 g H_2SO_4 + 100 mL distilled water under DC voltage of 10 V. Electrochemical exfoliation method has been developed as high yield as well as high-quality method and obtained graphene can be used in electrical and electronic devices.

2.2 Thermal chemical vapor deposition

Chemical vapor deposition process is used to synthesize the high-quality solid materials in which volatile precursors react and/or decompose on the exposed substrate. For the first time, Somani et al. [25] synthesized the few planar layer graphene by thermal CVD process using camphor. The authors used two horizontal furnaces, one for evaporation of camphor at 180 °C and in another furnace, it was pyrolyzed at 700–850 °C using Ar as a carrier gas. Ni sheets were used as a substrate on the second furnace. The deposited graphene layers on the Ni substrate were scraped and characterized using a high-resolution transmission electron microscope (HRTEM). However, this method could not produce a single graphene layer. The number of graphene layers was found to be 35 on the substrate as shown in Fig. 2.

Obraztsov et al. [26] has adopted the CVD method with a different source of carbon. They used the mixture of hydrogen-methane (92:8) gas at a pressure of 10.67 KPa. After activation of this mixture by DC discharge, the vapor was deposited on the Ni and Si substrate at 950 °C. It resulted in 1.5 ± 0.5-nm film after 15 min. They also observed that substrate material significantly affect the graphene deposition detected by a scanning tunneling microscope (STM). STM image of the deposited film (Fig. 3) shows that graphene on Si substrate consisted of many tiny grains whereas in Ni substrate graphene layers formed ridges of 2 μm. The authors reported that the disordered structure of graphitic film on Si substrate is due to the larger lattice mismatch between Si and graphene. Yu et al. [27] adopted the similar method and were able to produce 3–4 layers of graphene by controlling the segregation of carbon. This work was based on the concept of graphite segregation on the grain boundaries and surfaces of metals. The hydrocarbon gas was passed over the Ni substrate at 100 °C which resulted in decomposition of hydrocarbon molecule on Ni surface followed by carbon diffusion in the Ni. After 20 min of deposition, the substrate was cooled with optimized cooling rate (10 °C/s). These steps are presented in Fig. 4. The cooling rate was optimized based on the

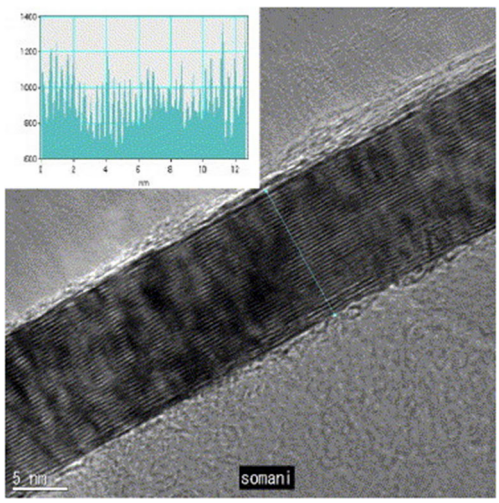

Fig. 2 HRTEM image of planar graphitic layer. Reprinted with permission from Ref. [25]

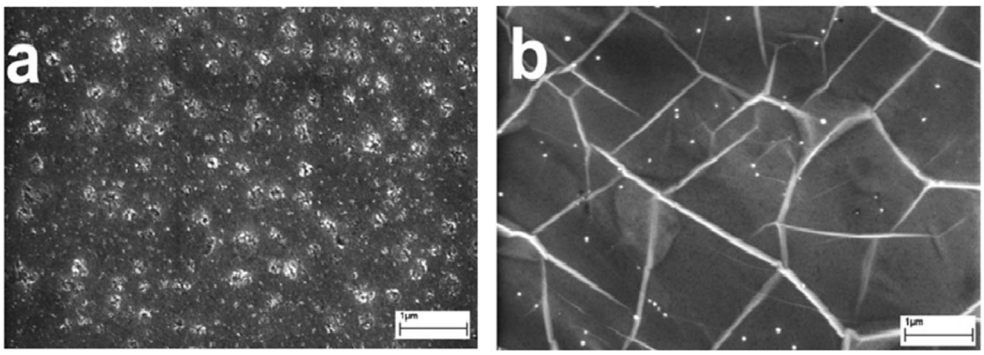

Fig. 3 SEM image of graphitic film on the **a** Si substrate and **b** Ni substrate. Reprinted with permission from Ref. [26]

segregation of C; extremely slow cooling rate resulted in the diffusion of C in the bulk whereas fast cooling rate caused reduction of C atom mobility to segregate. The graphene layers were detached from Ni in HNO_3 solution. Before etching away the Ni with HNO_3, graphene layer was covered with thin layer of silicon and glass.

Later, De Arco et al. [28] demonstrated that single-layer graphene can be produced by thermal CVD by optimizing the hydrocarbon gas content, gas flow rate, and temperature. They used 4-in. Si/SiO_2 wafer coated with 100 nm Ni film as a substrate. Ni coating was chosen because nickel and carbon have a favorable interaction which allows the epitaxial growth of carbon on Ni (111) surface. After Ni film deposition, the CVD process was carried out to deposit graphene using 600 sccm of H_2 up to 800 °C and methane gas at a flow rate of 100 sccm for 8 min. They found that diluted methane content plays an important role to produce single and few layers of graphene. The synthesized graphene was confirmed by the typical strong peaks at 1580 and 2690 cm^{-1} in Raman Spectra. The observed peaks correspond to G and G′ bands of graphene.

Thermal chemical vapor deposition technique is one of the effective technique to produce single and few-layer graphene films. This technique has also been used on single crystal material such as Ni to produce defect-free single-layer graphene [29].

2.3 Plasma enhanced chemical vapor deposition (PECVD)

PECVD is a process to deposit the gas (vapor) to a solid substrate. It uses electrical energy to convert the gas into plasma (ionized gas or other highly excited species). These highly excited species interact with the substrate and, depending on interaction deposition occur. PECVD is an excellent alternative for CVD due to its lower temperature requirement. Synthesis of graphene by PECVD was first reported in 2004 [30, 31]. The graphene sheets were synthesized in radio

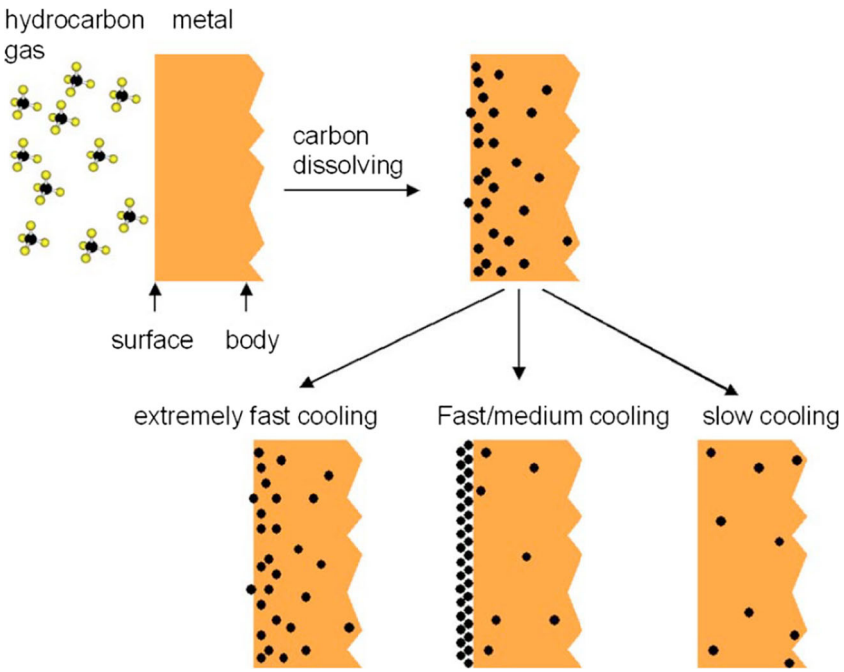

Fig. 4 Steps involved in graphene synthesis by segregation of C on Ni substrate. Reprinted with permission from Ref. [27]

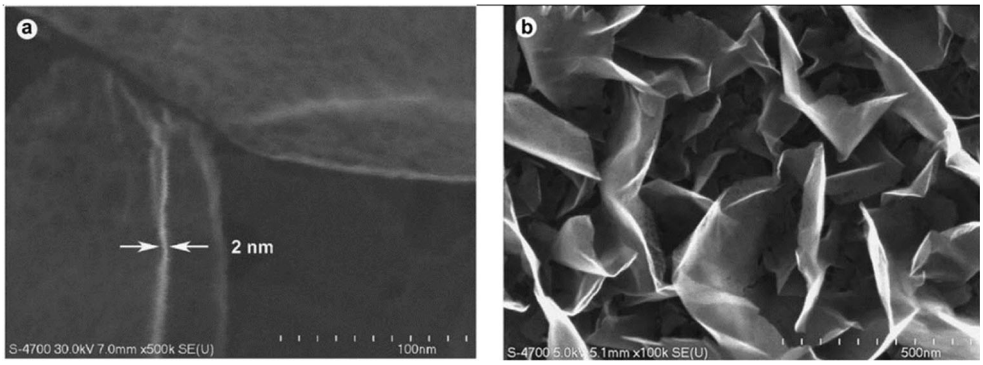

Fig. 5 **a** Higher magnification SEM image. **b** Low magnification SEM image of graphene on Si substrate at 40% CH_4. Reprinted with permission from Ref. [31]

frequency (13.56 MHz) PECVD system on a various substrate (Al_2O_3, SiO_2, Cu, Hf, Mo, Nb, Si, Ti, Ta, W, Zr, and 304 stainless steel). Methane was used for carbon source with a volume concentration range in H_2 atmosphere. The parameters, RF power (900 W), flow rate (10 sccm) and gas pressure (~ 12 Pa) were kept constant for all the substrates. While temperature and deposition time varied from 600 to 900 °C and 5 to 40 min respectively, based on substrates. The produced graphene sheets were characterized using SEM, HRTEM, and Raman spectrometer. The presence of characteristics G and G′ band on Raman spectra confirmed the crystalline graphene sheets. The observed 2-nm-thick graphene sheet is shown in Fig. 5.

Multilayer graphene nanoflake films (MGNF) on Si substrate was also synthesized by microwave plasma enhanced chemical vapor deposition [32]. For carbon source, methane was introduced after preheating the substrate in nitrogen plasma of 900 W of 5.33 KPa pressures. During deposition, microwave power was increased to 1300 W. The produced graphene SEM image is shown in Fig. 6. It showed knife-edge or a conical structural with 2–3 nm sharp edge. Apart from the shape of graphene, the authors found the growth rate was 1.6 μm/min and it was claimed to be ten times faster than the previously reported information.

PECVD method has been a versatile synthesizing technique for graphene deposition on any substrate. Thus, it expands the use of PECVD, and it has been used on various substrates such as Cu [33, 34], Ni [35, 36], and Co [37].

2.4 Other techniques

2.4.1 Thermal decomposition of SiC

It is one of the popular techniques for graphene synthesis. In this technique, graphene is grown epitaxially on single crystal of 6H-SiC. Graphene sheets were found due to etching of 6H-SiC by H_2 at a temperature range of 1250–1450 °C for 1–20 min. The number of resulted graphene layers highly dependent on temperature. In a similar approach, Rollings et al. [38] produced single-layer graphene by thermal decomposition of SiC. This method has been widely adopted for graphene synthesis [39–41]. Apart from laboratory-scale production, few issues have to be resolved such as layer thickness control and large area sheets to use this technique for industrial production.

2.4.2 The chemical method from graphene oxide

Formation of graphene oxide is the first step for this method. Graphene oxide formation was first reported in 1958 by Hummers and Offeman [42]. The authors successfully prepared the graphene oxide by stirring 100 g of graphite

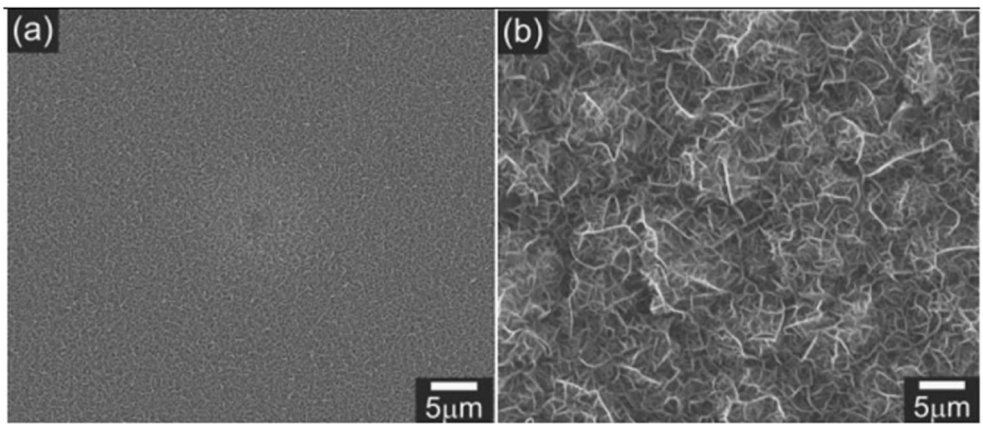

Fig. 6 SEM image of multi layered graphene deposited after **a** 40s and **b** 30 min. Reprinted with permission from Ref. [32]

Table 2 Other techniques for graphene synthesis

Process	Process material	Produced graphene form	Reference
Thermal decomposition of SiC at low temperature (750 °C)	200 nm Ni-coated 6H-SiC(0 0 0 1) substrate	Single to few layers	[49]
Ion implantation	500 nm Ni-coated Si/SiO_2 substrate	Single to 3 layers	[50]
Thermal decomposition	Single crystal Ru (0001) substrate	Periodic rippled layers	[51]
Unzipping of multiwall carbon nanotubes (MWNT)	Intercalation by Li and ammonia	Partially open tubes and graphene flakes	[52]
Unzipping of MWNT	Plasma etching	Coexistence of MWNT and single- to few-layer graphene nanoribbons	[53]
Unzipping of MWNT	Chemical exfoliation by H_2SO_4, $KMnO_4$, and H_2O_2 followed by reduction in NH_4OH and hydrazine solution	Oxidized edges and planes of the nanoribbons	[54]
CO gas reduction by Al_2S_3	Deposition of C on alumina (product by calcination of Al_2S_3)	Rippled and entangled few-layer graphene sheets	[55]
Graphene oxide reduction by solar radiation	Exposure of focused solar radiation on graphene oxide by convex lens for 2–3 min	1–2 nm thin graphene flakes	[56]
Edge-selectively functionalized graphene nanoplatelets by ball milling	Ball milling of graphite in the presence of different environment (H_2, dry ice and sulfur trioxide) for the different functional group	Folded and wrinkled few-layer functionalized graphene	[57]
Graphene flakes by multiple electrochemical exfoliations of graphite rod	Electrochemical cell consists of graphite (anode) and platinum (cathode) in protonic acid aqueous solution	Multilayered graphene (10–15 layers)	[58]

powders and 50 g of sodium nitrate ($NaNO_3$) into 2.3 L of sulfuric acid (H_2SO_4). The obtained mixture was kept in the ice bath and vigorously agitated. Subsequently, 300 g of potassium permanganate ($KMnO_4$) was carefully added to the suspension in order to maintain the temperature 20 °C. Then the ice bath was removed, and the suspension was held at 35 ± 3 °C for 30 min. During this period, the reaction occurred and the mixture became thick paste. In next step, 4.6 L of water gradually added into the paste, resulting in violent effervescence and raising the temperature up to 98 °C due to chemical reaction. The diluted solution kept at this temperature for 15 min followed by addition of 14 L of warm water. The resulted diluted solution was treated with 3% hydrogen peroxide to reduce the residual potassium permanganate. After hydrogen peroxide treatment, the warm suspension was filtered to produce bright yellow cake, which subsequently washed by 14 L of warm water. It formed a suspension of the graphitic oxide residue in the 32 L of water. After centrifugation and dehydration of suspension at 40 °C over phosphorous pentoxide, graphene oxide was obtained in the dry form.

Wu et al. [2] synthesized the graphene using chemical exfoliation method. After formation of graphene oxide using Hummers's method [42], graphene oxide was thermally exfoliated at 1050 °C for 30 s. The resulted thermally exfoliated graphene oxide was reduced by H_2 for 2 h at 450 °C in the environment of H_2 (100 mL/min) and Ar (100 mL/min). After reduction, it was stirred in a solution of N-methylpyrolidone

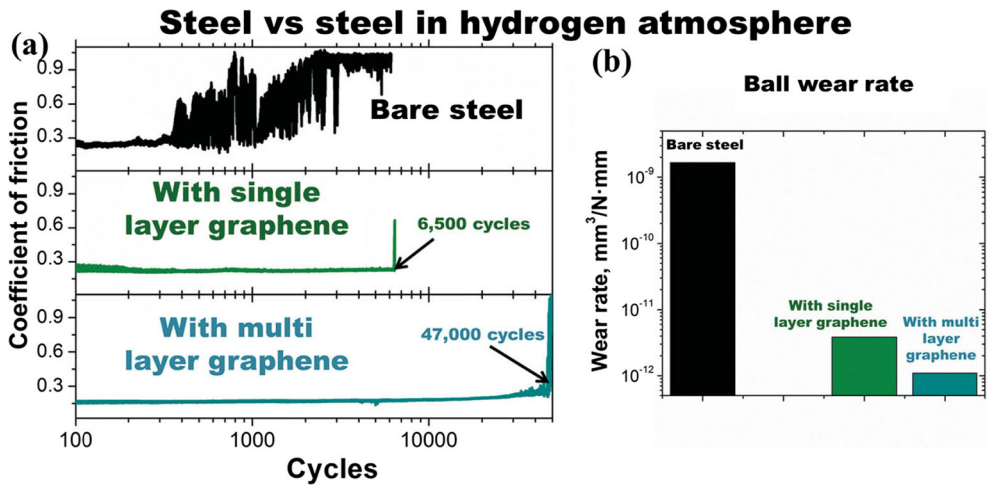

Fig. 7 **a** Coefficient of friction and **b** wear rate for bare steel, single-layer graphene, and few-layer graphene against steel ball as a counterpart. Reprinted with permission from Ref. [8]

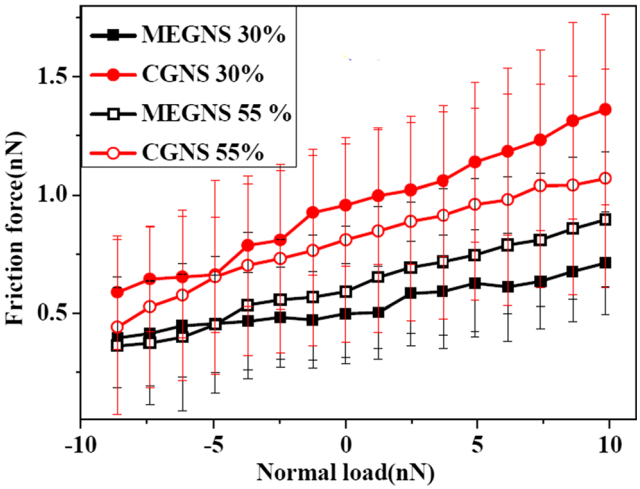

Fig. 8 Frictional force of AFM tip versus normal load at 30 and 55% R.H. for mechanically exfoliated graphene nanosheets (MEGNS) and CVD graphene nanosheets (CGNS) on SiO_2/Si substrate at ~25 °C. Reprinted with permission from Ref. [12]

followed by sonication. Finally, the thick multilayer graphene was separated by centrifugation and produced graphene layers.

In another approach, Sahu et al. [43] have developed a chemical route to extract graphene from graphene oxide by Hummers' method [42]. First, this GO was exfoliated by ultrasonication in distilled water. This exfoliated GO is reduced by the addition of hydrazine hydrate followed by refluxing the suspension in the oil bath at 90 °C for 2 h stirring. These finally results in the black-colored precipitate of graphene.

Later, Marcano et al. [44] demonstrated improvement in the Hummers' method by performing the reaction in a 9:1 mixture of H_2SO_4/H_3PO_3. The addition of phosphoric acid did not only increase the yield by a higher degree of the oxidation process of graphitic structure but it also produced more intact graphitic basal plane. The higher yield and regular graphene oxide lead to the application of this improved Hummers' method for several graphene studies [45–48].

Some of the other methods are listed in Table 2.

3 Tribology of graphene and graphene composites

Various frictional studies [8, 12, 59] on graphene indicate that graphene can be promising material in the field of tribology. Berman et al. [8] demonstrated the extraordinary properties of single-layer and multilayer graphene using the ball-on-disc tribological test. Single-layer and multilayer graphene with steel (400C grade) substrate were tested using 9.5 mm diameter steel (400C) as a counterpart. The test was conducted with 1 N of the normal load at a speed of 60 rpm in dry hydrogen (90 KPa) at room temperature. Single-layer graphene deposited steel substrate lasted for more than 6400 cycles which is much better than other solid lubricants, such as diamond-like carbon and MoS_2. Furthermore, the multilayer graphene deposited steel substrate provided lower friction for 47,000 sliding cycles. The similar trend was observed for wear rate as shown in Fig. 7.

The decrease in friction with an increase in graphene layers on Si and SiC substrate was also observed using frictional force microscopy techniques [59, 60]. Lee et al. [59] reported that the decrease in friction with increase in graphene layers does not depend on the scan speed and load. The authors proposed that rippling edge effect can be the possible explanation for the observed trend. Since the single layers are found to have ripples [61, 62], and during characterization, AFM tip needs to provide extra energy to push the ripples forward. As the number of graphene layers increases, the ripple formation can be lesser which leads to lower friction. Later, this ripple edge effect hypothesis was confirmed by the same group [63]. The authors used graphene on Si substrate, free-standing graphene membrane, and mica substrate. Graphene on Si substrate and free-standing graphene sheets showed the decrease in friction with an increase in graphene layers. But graphene on mica substrate did not show thickness dependency on friction; it is because graphene and mica had strong adhesion which did not allow to form ripples. It suggests that substrate plays a significant role for frictional properties of graphene. Defects are also one of the determining factors for frictional

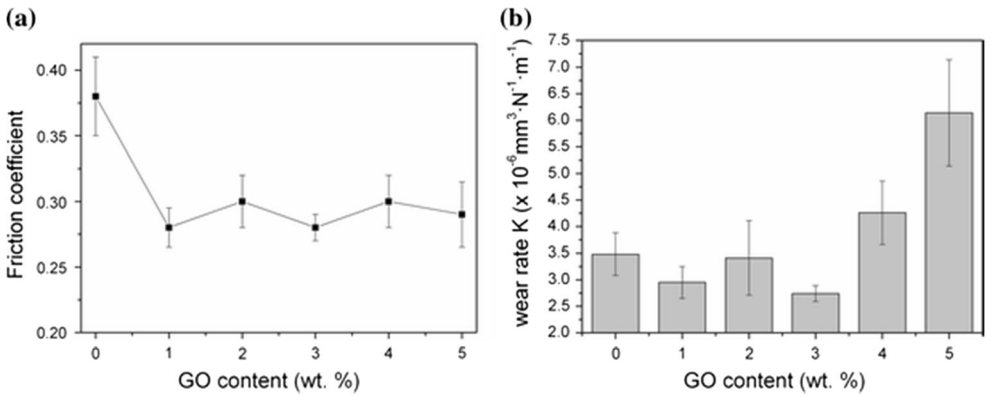

Fig. 9 Effect of graphene oxide content on polyimide/graphene oxide composites. **a** Friction coefficient and **b** wear rate. Reprinted with permission from Ref. [48]

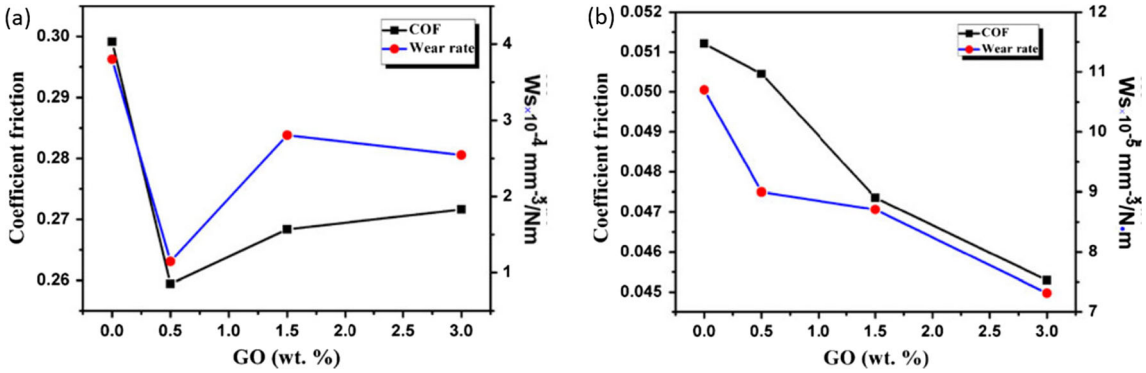

Fig. 10 Variation of coefficient of friction and wear rate of graphene oxide/nitrile rubber with different content of graphene oxide (GO) for **a** dry condition and **b** water lubricated condition. Reprinted with permission from Ref. [68]

properties of graphene. Peng et al. [12] studied the frictional properties of graphene produced by different methods. The authors observed that mechanically exfoliated graphene shows high lubrication and zero wear under high pressure due to defect-free graphene layers. Due to defects in CVD graphene nanosheets (CGNS), it decreased the friction and wear properties. This effect is shown in Fig. 8 which represents the variation of frictional force with a normal load in 30 and 55% relative humidity. The frictional force on MEGNS increased with increase in relative humidity, whereas the opposite trend was observed on CGNS. The possible reason for this behavior is due to the presence of defects on CGNS can cause reduction in the hydrophobicity compared to MEGNS. This slight reduction in hydrophobicity can lower the friction force on CGNS by increasing humidity.

The low coefficient of friction and lesser wear rate promote the importance of graphene in the field of tribology. These tribological properties can be utilized by manufacturing the self-lubricating nanocomposites and as an additive in lubricant oil. Composite materials have the combination of properties of constituents. In this regard, self-lubricating nanocomposites materials have been using in the field of automotive, space, and marine industries [64–66] and graphene-based self-lubricating materials can be promising materials. Various studies have been carried out on graphene nanocomposites using polymer, metal, and ceramic material as a matrix. The following sections describe the role of graphene as a reinforcement in various matrix materials and as an additive in lubricant oil.

3.1 Polymer-matrix composites reinforced by graphene

Graphene is an emerging material for synthesizing polymer composites. However, the hydrophobic nature of graphene [67] and poor compatibility of pristine graphene with polymers make it difficult to use for polymer-matrix composites [68]. To overcome these issues, graphene has been used either in the form of graphene oxide [48, 68–70] or by using some modifier to disperse graphene uniformly [9, 71, 72]. It has been also found that modifier does not only help to dissolve graphene, but it also provides better tribological properties than the pristine graphene in polymer composites [73, 74]. However, very few studies have been carried out on the tribological performance of polymer-matrix composites reinforced by graphene or graphene oxide. In one of the study, Liu et al. [48] investigated the tribological properties of polyimide/graphene oxide nanocomposites. The authors prepared the graphene oxide nanosheets by improved Hummers' method [44] as described in the synthesis of graphene section. They stated that oxygen-containing functional groups on graphene

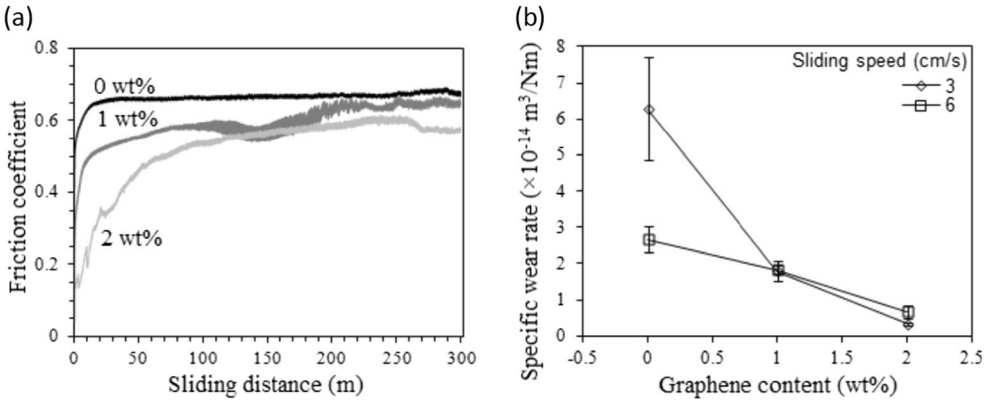

Fig. 11 **a** Coefficient of friction and **b** specific wear rate for epoxy and epoxy/graphene composites. Reprinted with permission from Ref. [9]

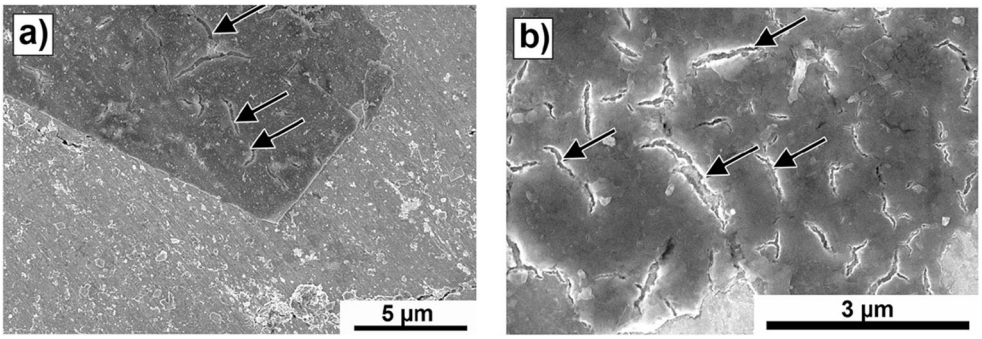

Fig. 12 SEM micrographs of worn surface. **a** Arrow indicating the microcracks on 5 vol.% graphene-AA6061 composite and **b** arrow indicating the graphene layers on 10 vol.% graphene-AA6061 composite (applied load 1 N). Reprinted with permission from Ref. [85]

oxide avoid stacking and regraphitization and the produced graphene oxide had nanosheets with corrugations. This graphene oxide was added and ultrasonicated to phenylethynylphthalic acid and methyl alcohol solution. The obtained solution was painted on a steel block and dried at 100, 200, 300, and 375 °C for 1 h, respectively. Tribological tests were carried out under dry sliding condition against GCr15 steel. The results are shown in Fig. 9. It can be clearly seen that with the addition of graphene oxide the COF goes down drastically while wear rate limits the graphene oxide content to 3 wt.%. The authors observed a uniform transfer layer on composites compared to polyimide and they suggested that addition of graphene oxide strengthened the transfer layer as well as improved the adhesion of transfer layer on the counter surface. Thus, the uniform and stable transfer layer altered the wear mechanism and provided better tribological properties. The same group conducted the study on the graphene oxide/nitrile rubber nanocomposites [68]. Nanocomposites were prepared by solution mixing method using nitrile rubber (NBR) and graphene oxide synthesized by improved Hummers' method. The same trend was observed as in the polyimide/graphene oxide as shown in Fig. 10. The COF and wear rate goes down by the addition of graphene oxide. In dry condition, the COF reduced from 0.3 to 0.26 by addition of 0.5 wt.% graphene oxide in nitrile rubber and further addition of graphene increased the COF. These values indicate that 0.5 wt.% is the optimized amount of graphene for dry condition. However, underwater lubricated condition (Fig. 10b), COF was continuously decreasing by addition of graphene. It suggests the graphene content was not optimized and there was possibility of further lowering the friction by adding more graphene.

Tai et al. [69] have also observed the improvement in the tribological properties of ultrahigh molecular weight polyethylene (UHMWPE) by adding graphene oxide. The authors found the wear rate of graphene oxide/UHMWPE nanocomposites was 1.0×10^{-5} mm^3 N^{-1} m^{-1} with 3 wt.% graphene oxide compared to 1.7×10^{-5} mm^3 N^{-1} m^{-1} wear rate of the only UHMWPE. However, the average COF slightly increased from 0.095 to 0.15 with addition 3 wt.% of graphene in UHMWPE. The authors suggested that the slight increase in COF was due to increase in surface roughness and shear strength by graphene oxide addition. Though there is a slight increase in COF, the significant decrease in wear rate makes the graphene oxide/UHMWPE promising material for hip and knee joint implants.

Graphene-modified epoxy composites have also found to be enhanced tribological properties. Khun et al. [9] studied the effect of graphene content on epoxy composites. They prepared the composites by the dispersion of epoxy resin (Epolam 5015) and graphene sheets, which mechanically stirred at 1500 rpm for 1 h. After introducing the hardener into the dispersion, the mixture was degassed followed by molding. The final composites were prepared by the curing the molded specimen in two stages, first at room temperature for 24 h then at 80 °C for 2 h. The tribological properties of

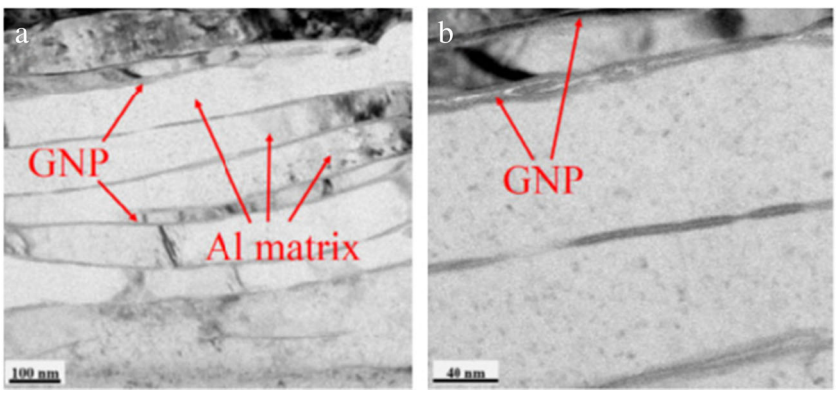

Fig. 13 TEM micrograph of Al-1 wt.% graphene nanoplates at different magnification. Reprinted with permission from Ref. [86]

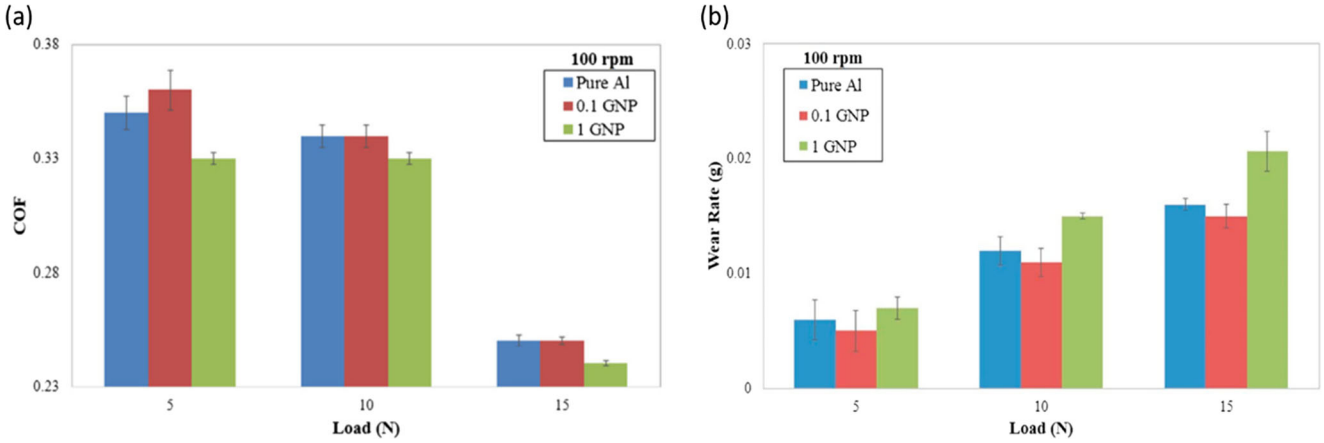

Fig. 14 **a** Coefficient of friction and **b** wear rate variation with normal load for pure Al, 0.1 and 1 wt.% graphene nanoplates. Reprinted with permission from Ref. [86]

composites were investigated using a ball-on-disc tribometer. In the experiment 100CR6 steel ball of 6 mm diameter was used as a counterpart. The COF was found to decrease with increase in graphene content as presented in Fig. 11a. Fig. 11b shows the specific wear of epoxy and epoxy/graphene composites at two different sliding speeds. When the graphene content is zero, the specific wear rate was high at both the sliding speed. After addition of graphene, the wear rate decreased. The decrease in specific wear rate suggests that epoxy graphene composites have superior tribological properties than epoxy.

Apart from tribological studies, polymer-matrix nanocomposites reinforced by graphene have been shown better mechanical, dielectric, thermal, and electrical properties [70, 72, 75–77]. Tang et al. [72] have shown the effect of graphene on polyvinyl alcohol. Rhodamine B (RhB) was used to prepare suspended graphene aqueous colloid due to the cation-π and π-π interaction between graphene and RhB. The authors observed that with the addition of 1% of RhB-graphene, the tensile strength, and modulus of the composites were increased by 178 and 139% respectively. Graphene has also found to improve dielectric constant of barium titanate fibers in polymer composites [75]. Wang et al. [75] observed highest dielectric constant with a combination of barium titanate and graphene platelets in polydimethyl siloxane matrix. Graphene-based polymer nanocomposites have been found to have high thermal conductivity and advantage of improving barrier properties compared to polymer-matrix reinforced with carbon nanotubes [70, 76]. These studies suggested that the polymer-matrix composites reinforced by graphene or graphene oxide have the potential to be used in various fields such as bearing, hip, and knee joints. However, the chemistry between graphene and different polymers has to be understood vigorously. Understanding of chemistry will play a vital role to distribute graphene uniformly and also to optimize graphene content on the polymer as it can be seen that graphene content is limited up to ~ 3 wt% in the polymer-matrix.

3.2 Metal-matrix nanocomposites reinforced by graphene

Unique properties of graphene such as high strength, low weight, and lubrication make the graphene suitable material for reinforcing the metal-matrix. The uniform distribution and structural integrity of graphene in the metal-matrix have been a stiff challenge in developing metal-matrix composites reinforced by graphene [78, 79]. Due to high surface area, graphene sheets are converted into clusters and behaves like particulate graphite particles, and it limits the graphene content in a metal-matrix. As graphene is a new material, very few tribological studies have been carried out on metal-matrix nanocomposites reinforced by graphene. Among the other metals and alloys, aluminum alloys have been the favorite for manufacturing composites due to high strength to weight ratio, corrosion resistance, and superior tribological properties [78, 80–84]. Ghazaly et al. [82] investigated the effect of graphene on the wear rate of self-lubricating AA2124

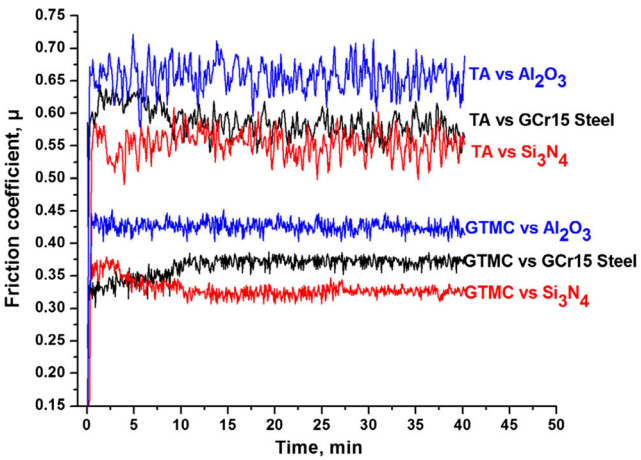

Fig. 15 Coefficient of friction variation with time for TiAl (TA) and multilayered graphene composites TiAl (GTMC). Reprinted with permission from Ref. [10]

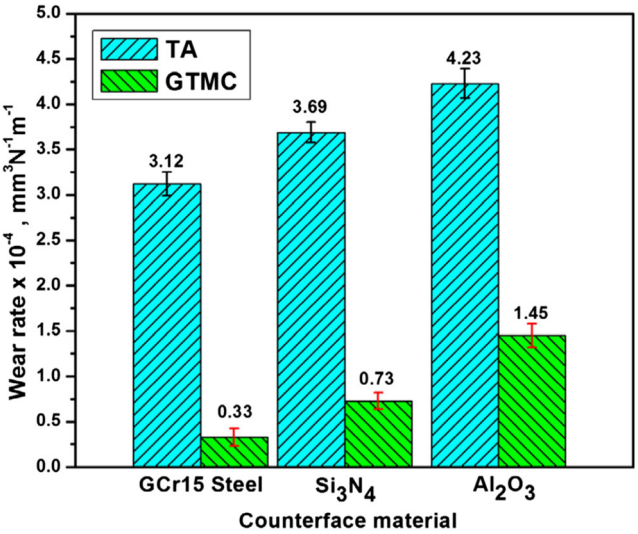

Fig. 16 Wear rate for TiAl (TA) and multilayered graphene composites TiAl (GTMC) versus different counterpart. Reprinted with permission from Ref. [10]

aluminum alloy composites. The composites were prepared by mixing the AA2124 powder and graphene platelets followed by cold compaction at 525 MPa pressure. The minimum wear rate found to be 1×10^{-4} mm^3 N^{-1} m^{-1} for 3 wt.% graphene compared to 0.35×10^{-4} mm^3 N^{-1} m^{-1} wear rate of 5 wt.% graphene composites. The authors also reported that 5 wt.% graphene composites have several parallel grooves compared to 3 wt.% graphene composites. This severe wear explains the increase in wear rate. In one of the similar study on AA6061-graphene composites, Wozniak et al. [85] observed the graphene layers on the scratched surface which explains the mechanism of self-lubrication and low wear rate. The authors prepared the composites by mixing the AA6061 powder and graphene followed by spark plasma sintering at 500 °C with a heating rate of 225 °C/min in argon atmosphere. Tribological tests were carried out on ball-on-disc setup 0.1 m/s sliding speed for 1000 revolution, and 100Cr6 steel was used as a counterpart. With a load of 1 N, 5 vol.% graphene-AA6061 composite showed higher wear rate (5.5×10^{-2} mm^3/m) compared to wear rate (0.15×10^{-2} mm^3/m) of 10 vol.% graphene-AA6061 composite. The resulted worn surfaces are shown in Fig. 12. The microcracks were present on the 5 vol.% graphene-AA6061 composite surfaces as indicated by arrows in Fig. 12a, whereas 10 vol.% graphene-AA6061 composite surfaces had uniform graphene transfer layers formed on the worn surface (Fig. 12b). These lubricant layers of graphene explain the lower wear rate in 10 vol.% graphene-AA6061 composite.

Tabandeh-Khorshid et al. [86] carried out similar studies on pure aluminum matrix reinforced by graphene nanoplates. The authors first prepared the slurry of graphene nanoplates by dispersing it in 99.5% anhydrous ethanol by ultrasonication. Then the slurry and aluminum powder were ball milled for 6 h at 500 rpm to prepare 1 wt.% graphene composites. After drying, powders were consolidated by cold compaction with 200 MPa at room temperature followed by hot compaction at 525 °C. TEM study revealed the expected layered microstructure due to change in morphology of aluminum to flakes during ball milling. TEM micrographs are presented in Fig. 13. It was observed that 1 wt.% graphene composites had a better COF in comparison with other samples as represented in Fig. 14a. The low COF was observed in 1 wt.% graphene composite due to the formation of graphene films on the surface during pin on disc test. However, wear rate was found to be higher for 1 wt.% graphene composites. Further, the authors obtained that aluminum had the highest hardness (92.48 ± 0.45 HR$_F$) while the 1 wt.% graphene composites aluminum had the lower hardness (86.08 ± 0.58 HR$_F$). This lower hardness value explains reason for higher wear rate of 1 wt.% of graphene composites, as it is well-known that materials with lower hardness have higher wear rate.

It has been also observed that graphene can reduce the wear of Al-graphene composites at high temperature [87]. The authors found that the wear rate of Al-2 vol.% graphene composites at 200 °C was reduced by 40% compared to room temperature under the same testing parameters (1 N normal load with a speed of 100 RPM against the 3 mm alumina ball for 30 min and surface roughness was 0.6 μm). This result is contrary to the fact that materials wear out more by increasing temperature due to softening. However, the authors suggested

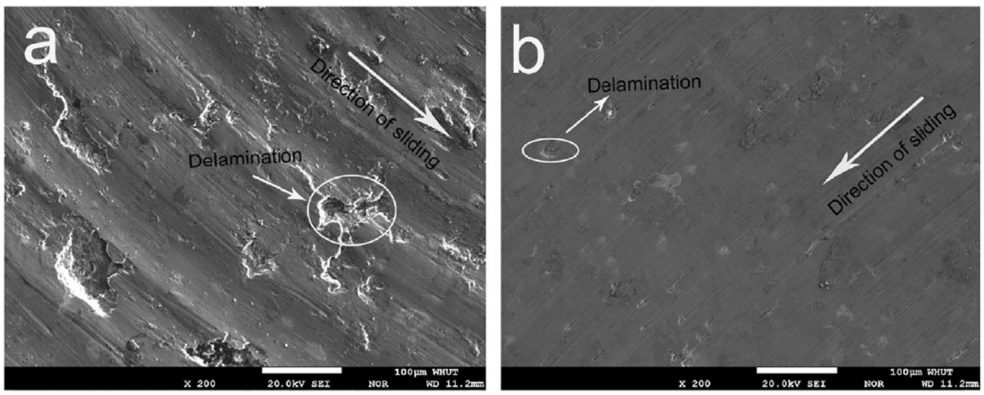

Fig. 17 EPMA micrograph of worn surface for **a** TiAl vs. GCr15 steel and **b** graphene/TiAl composites vs. GCr15 steel. Reprinted with permission from Ref. [10]

Table 3 Carbonaceous material in silicon nitride-based nanocomposites [11]

Type of carbon addition	Amount, wt.%	COF
None	0	0.77 to 0.81
Graphite	10	0.83
Carbon nanotube	3	0.77 to 0.81
Carbon black	3	0.72
Graphene	3	0.52

two possible explanation: (i) localized sintering and further densification during tribological testing at 200 °C and (ii) graphene can for a film on the surface and prevent the oxidation of underlying Al grains that can reduce abrasive wear due to the formation of hard Al_2O_3.

Xu et al. [10] observed the drastic improvement in the tribological properties of TiAl-matrix composites reinforced by multilayer graphene. TiAl alloy consisted of Ti, Al, Nb, Cr, and B powders with a molar ratio of 48:47:2:2:1 and multilayer graphene had an average thickness of 40 nm and average lateral dimension of 50 μm. The powders with graphene of 3.5 wt.% were ball milled for 8 h at 80 rpm followed by spark plasma sintering at 1100 °C with a heating rate of 100 °C/min and 50 MPa pressure. The tribological test was carried out using ball-on-disc arrangement. GCr15 steel, Si_3N_4 and Al_2O_3 balls were used as a counterpart at 10 N load with a speed of 0.2 m/s. The COF were found to be decreased by a factor of 4 whereas the wear rate decreased by 4 to 9 times of magnitude. The COF and wear rate variations are shown in Fig. 15 and Fig. 16, respectively. The improved tribological properties were due to the formation of the lubricious film during wear test, and it can be seen in the EPMA micrograph of worn surfaces against GCr15 steel as shown in Fig. 17. The worn surface of TiAl showed many delaminations whereas graphene consisting composites had a smooth surface. Similar observation was made for Al_2O_3 and Si_3N_4 balls as a counterpart.

Effect of graphene was also observed in the Cu metal-matrix. Chmielewski et al. [88] prepared the Cu-matrix composites by mixing the Cu powders and graphene (1–5 nm) in a planetary ball mill for 4 h at 100 rpm followed by spark plasma sintering in vacuum at 950 °C with heating rate 100 °C/min and 50 MPa of pressure. Three composites were prepared with 3, 5, and 10 vol.% of graphene. The tribological properties were investigated using ball on plate tribosystem. The COF and wear scar diameter were found to be decreased nearly by 2 times for 3 wt.% graphene composites in comparison with Cu and as the graphene content increased the COF and wear scar diameter further decreased.

Hu et al. used laser to synthesis graphene oxide-Ti composite coating [79] and graphene-Ti composite coating [89]. Laser sintering provides rapid heating and cooling process, thus avoiding the reaction between carbon (graphene) and Ti matrix. The authors developed the coating on AISI 4140 steel sample by dropping the ethanol solution consisted of graphene and Ti powder. After, natural drying of ethanol, laser sintering was carried out by IPG fiber laser system at the frequency of 50 kHz. Laser sintering was carried out between 920 °C and melting point of Ti (1600 °C), since the 920 °C is the eutectic temperature at which Ti reacts with carbon. However, during sintering, the rapid cooling does not allow TiC formation after moving away the laser beam. The observed hardness value of graphene oxide-Ti coating and graphene-Ti coating were 13.5 and 7.9 GPa, respectively. These values are significantly higher than the hardness of sintered Ti coating, i.e., 4 GPa. These studies were focused toward mechanical properties. However, these suggest that laser sintering can be used to synthesize graphene-metallic composites that avoid major problem of reaction between carbon (graphene)–metals and it also helps to achieve uniform dispersion of graphene in the metal-matrix.

It can be seen that different graphene nanocomposite materials exhibit different tribological properties as per the metal-matrix. Thorough study is required to understand the interaction between graphene and metals. Knowledge of interaction between graphene and metals will help to understand the self-lubrication mechanism, and interactional studies can also be helpful to determine the factors which affect uniform distribution of graphene in a metal-matrix.

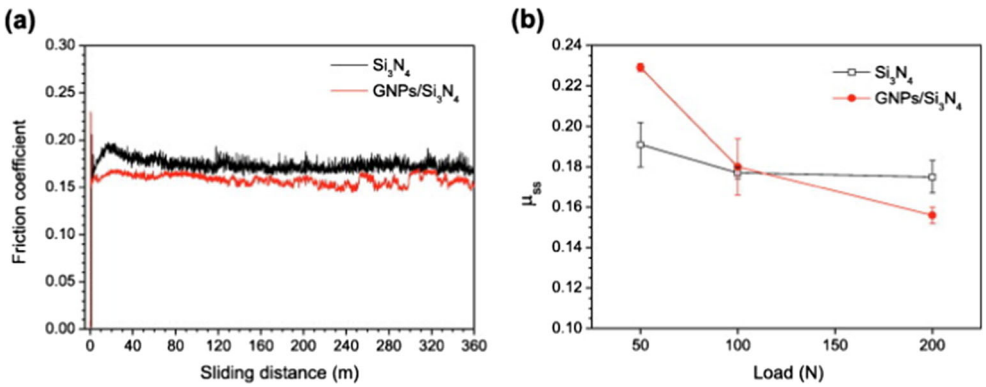

Fig. 18 **a** Coefficient of friction variation at 200 N and **b** steady-state friction coefficient (μ_{ss}) vs. load for Si3N4 and GNPs/Si_3N_4 material. Reprinted with permission from Ref. [91]

3.3 Ceramic-matrix composites reinforced by graphene

Ceramic materials with better tribological properties are in demand to avoid mechanical failure and improve the life of components in mechanical assemblies. Ceramic composites have their own advantage over the polymer and metal-matrix composites. The polymer-matrix composites have poor thermal stability, have lower hardness, and are also prone to certain chemical reactions while the metal-matrix composites are prone to corrosion in the sensitive environment [90]. A considerable amount of tribological studies has been carried out on ceramic composites such as Al_2O_3, Ni_3Al, and Si_3N_4 reinforced by graphene [11, 90–94]. In 2010, Prfeifer et al. [11] studied the tribological properties of silicon nitride-based nanocomposites with various carbonaceous materials. Composites were synthesized by powder metallurgy route. First, the powders 90% Si_3N_4, 4 wt.% Al_2O_3, and 6 wt.% Y_2O_3 with carbonaceous materials were milled using zirconia balls. Green compacts were obtained by pressing at 220 MPa followed by oxidizing treatment at 400 °C. Polyethlyleneglycol was used as a binder. Final composites have been achieved by hot isostatic pressing at 1700 °C in nitrogen atmosphere. The tribological test was performed at room temperature by ball-on-disc tribosystem in which silicon nitride ball was used as a counterpart. Among the various carbonaceous material, graphene remarkably showed the minimum COF as shown in Table 3. The addition of 3 wt.% graphene lowers the COF coefficient to 0.52 in comparison with pure silicon nitride which has ~ 0.8 COF.

A similar study was carried out on graphene/silicon nitride nanocomposites by Belmonte et al. [91]. First, the powders of Si_3N_4, 2 wt.% of Al_2O_3 and 5 wt.% Y_2O_3, and graphene nanoplatelets were dispersed in isopropanol and mechanically stirred. After drying the mixture, 20 mm diameter disc with 3 wt.% graphene was prepared by spark plasma sintering at 1625 °C with a pressure of 50 MPa. Ball on plate reciprocating tests were conducted with Si_3N_4 balls as counterpart and isooctane was used for lubrication. COF (μ) at 200 N was found to be lesser for graphene composites as shown in Fig. 18a. Whereas at 50 N, the steady-state COF (μ_{ss}) was found to higher for composites (Fig. 18b). The authors reported that 50 N, the debris (graphene and matrix material) covered a small area of the composite surface whereas at 200 N the wear scars were completely covered by debris. Therefore, at 200 N, continuous supply of exfoliated graphene led to low COF which is confirmed by the presence of graphene on a surface in the FESEM micrograph as shown in Fig. 19. However, Hvizdos et al. [92] and Balko et al. [93] observed no decrease in COF with 3 wt.% graphene in silicon nitride nanocomposites at room temperature. The authors reported that

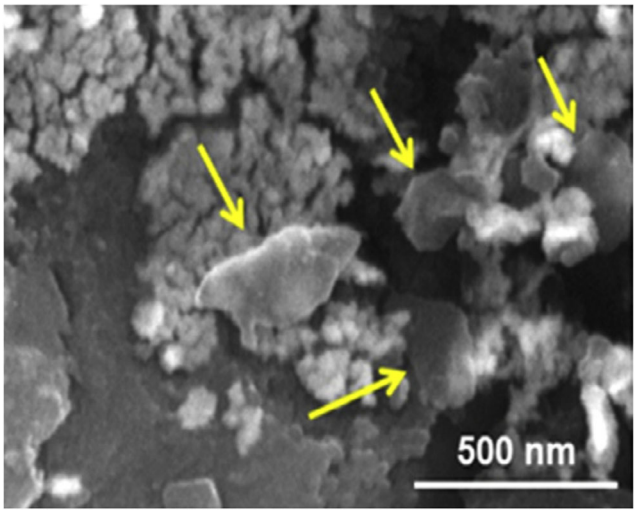

Fig. 19 FESEM micrograph of the worn surface of composite tested at 200 N. Arrows indicate the graphene debris. Reprinted with permission from Ref. [91]

graphene made the densification challenging and they found porosity in the samples as shown in Fig. 20. The presence of porosity could be the possible reason of no change in COF.

Alumina composites reinforced by graphene have also found better tribological properties. Gutierrez-Gonzalez et al. [94] studied the wear effect of graphene/alumina nanocomposites. Composites were prepared by spark plasma sintering at 1500 °C with a heating rate of 100 °C/min and pressure of 80 MPa. Wear properties were characterized by ball on plate with reciprocating motion with alumina ball as a counterpart. The load and sliding velocity were 20 N and 0.06 m/s respectively. The COF was reduced by ~ 10% and wear rate was reduced by ~ 50%. COF variation and wear rate are presented

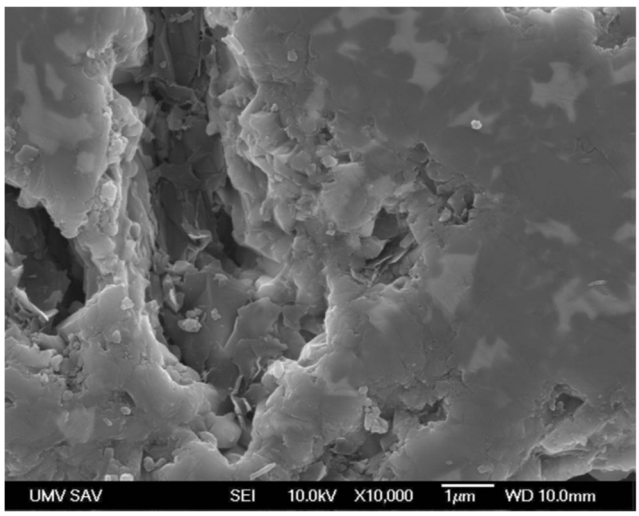

Fig. 20 Pores and uniformly distributed graphene flakes in the polished sample of 3 wt.% graphene of silicon nitride-based nanocomposites. Reprinted with permission from Ref. [92]

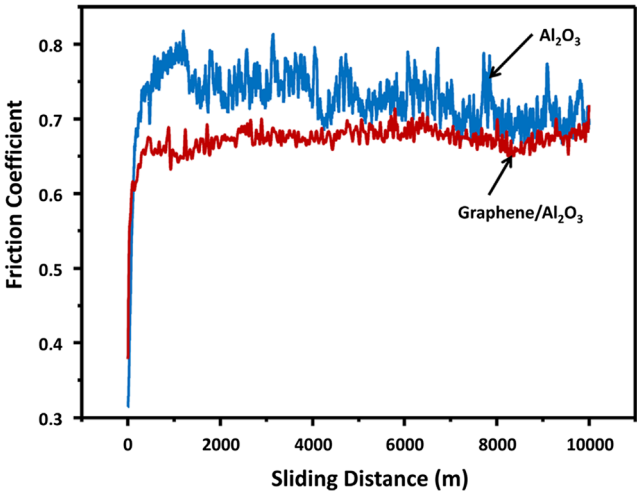

Fig. 21 Coefficient of friction variation for Al_2O_3 and graphene/Al_2O_3 composites. Reprinted with permission from Ref. [94]

in Figs. 21 and 22, respectively. The authors stated a mechanism that during tribological test, counterpart eroded the graphene aggregates from the composites and adhered to the surface. This lubricating and protective graphene films between counterpart (alumina) and composites improved the tribological performance.

Zhang et al. [95] also obtained similar results on spark plasma sintered Al_2O_3-graphene composites. They observed that 0.5 vol.% of graphene, wear volume and friction decreased by ~ 65 and ~ 25%, respectively. These studies suggested that formation of protective graphene tribofilm on wear surfaces decreased friction and wear. Several other studies showed that graphene is a suitable material for improving tribological properties of ceramic composites [90, 91, 96]. Apart from the tribological properties, graphene reinforcement in the ceramic-matrix is promising for better mechanical and various functional properties [97–101].

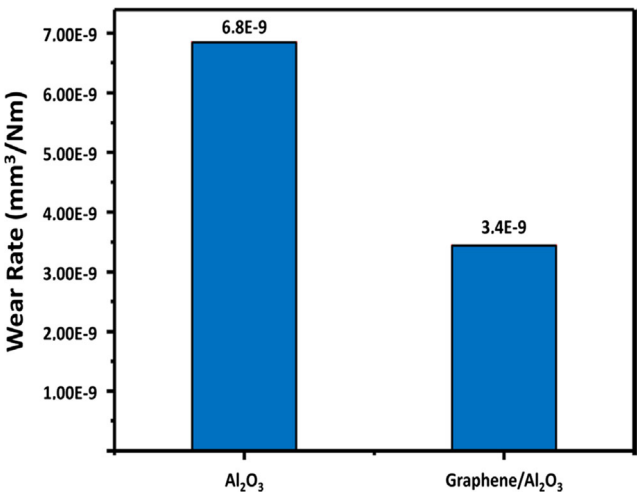

Fig. 22 Wear rate for Al_2O_3 and graphene/Al_2O_3 composites after 10 km of wear test. Reprinted with permission from Ref. [94]

3.4 Graphene as an additive in lubricant oil

In addition to graphene-reinforced composites material, lubricious nature of graphene can also be advantageous as an additive to lubricant oil. Prior to addition in oil, graphene requires modification to change the hydrophobic to hydrophilic nature for uniform suspension. Currently, two main approaches are being followed to develop uniform suspension of graphene platelets in lubricant oil. One is the use of graphene platelets and effective dispersant. Graphene platelets have been proven to effective additives as it contains hydroxyl and carboxyl functional group at graphene sheet edges as presented in Fig. 23. These functional groups make the graphene platelets strongly hydrophilic [103, 104].

The addition of effective dispersant helps to form stable suspension by embracing one nanoparticle to repel another in the oil [105, 106]. Huang et al. [105] have used this approach to investigate the tribological properties of graphite nanosheets as an oil additive. They prepared the graphitic sheet of 500 nm diameter and 15 nm thick by ball milling and dispersed in paraffin oil with the help of surfactant span-80. Tribological properties were examined using four-ball tester with the rotating speed of 1200 rpm under a constant load of 245 N for 30 min. They found that with the addition of 0.01 wt.% graphitic nanosheets, the COF was decreased by ~ 80% in comparison with pure paraffin oil as shown in Fig. 24. The authors stated that the reduction in the contact area of the rubbing surface due to the presence of graphitic nanosheets resulted in improved tribological properties. It was confirmed by the presence of deposited nanosheets on the rubbing surface presented in Fig. 25.

The other approach to obtain uniform dispersion is the modification of the graphene nanoplatelets with a proper modifier such as stearic acid, sodium dodecyl benzene sulfonate. Lin et al. [104] reported that the stearic acid and oleic acid are the most suitable modifiers for graphene nanoplatelets. The modification was carried out by sonication of graphene nanoplatelets with stearic acid and oleic acids (mass ratio 3:5) in cyclohexane. The obtained suspension was stirred and refluxed at 80 °C for 5 h. After cooling, the products were filtered and dried at 100 °C under vacuum. For the tribological test, the modified graphene platelets were dispersed in the 350SN base oil and tribological properties were measured by four-ball tribosystem. The test was conducted with the rotating speed of 1200 rpm under a constant load of 147 N for 60 min at 75 ± 2 °C. The results were compared with the modified graphite flakes as shown in Fig. 26. It can be seen that the wear rate and COF is the minimum for oil with modified graphene platelets (0.075 wt.%). A similar study with 0.02–0.06 wt.% oleic acid-modified graphene in gear oil (polyalphaolefin-9) have reported the reduction in wear scar diameter and COF by 14 and 17%, respectively [107].

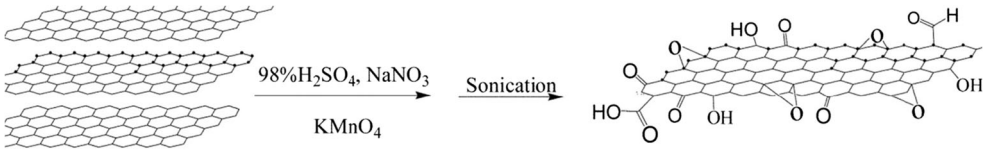

Fig. 23 Functional group on graphene by oxidation. Reprinted with permission from Ref. [102]

Eswaraiah et al. [56] demonstrated the improvement in the tribological properties of graphene-based engine oil without any surface modification. The authors first prepared the graphene oxide by modified Hummers' method, and then they used focused solar radiation to reduce graphene oxide into ultrathin graphene. The suspension was prepared by mixing the graphene and N-dimethylformamide to obtain 0.02 mg/mL concentration of graphene followed by dispersion of different amount of graphene in commercial engine oil. The tribological properties were tested using four-ball tester. The drastically improvement was observed with 0.025 wt.% graphene addition as shown in Fig. 27. For 0.025 wt.% graphene in engine oil, the COF and scar diameter were decreased by 80 and 33% respectively whereas the load carrying capacity of the oil was increased by 40%.

In addition to graphene, graphene oxide has also found to be an excellent additive in lubricant fluid as it is hydrophilic. However, graphene oxide also requires either dispersant or a proper modifier for uniform dispersion. Senatore et al. [108] studied the graphene oxide nanosheets as additive in mineral oil. It was observed that addition of 0.1 wt.% graphene oxide reduced the average COF by 16–20% and wear scar diameter was also decreased by 12, 27, and 30% in the boundary, mixed, and elastohydrodynamic regime respectively. Due to hydrophilic nature of graphene oxide, it can also be suspended in water-based lubricant [109, 110]. Graphene oxide nanosheets as water-based lubricant have found to have superior anti-wear ability and lower COF compared to water with oxide carbon nanotubes (CNTs-COOH) and the worn counterpart ball surface was also found to be smoother than the oxide CNTs [109]. Kinoshita et al. [110] tested the applicability of graphene oxide monolayer as water-based lubricant. They found that 1 wt.% addition of graphene oxide in water-based lubricant provided the lower COF approximately 0.05 and no significant surface wear was observed after 60,000 cycles of tribological test.

All the studies described above have suggested a possible mechanism by formation of thin protective graphene layers between rough surfaces. The mechanism can be understood by the schematic shown in Fig. 28. Without any solid additive, oil provides boundary lubrication. With optimized amount of graphene addition, a protective layer of graphene can form on the rough surfaces (Fig. 28b) results in mixed lubrication and improves the anti-wear properties. However, with an excess amount of graphene in the oil, the oil film can become discontinuous due to excess graphene and graphene acts as a third body. The absence of oil film lowers the tribological properties. Optimization of graphene content is the key to obtain a mixed lubrication condition. Thus, improving the tribological performance of lubricant oil with graphene suspension.

4 Other application of graphene

Apart from extraordinary mechanical and tribological properties, graphene has superior electrical, optical, and thermal properties that can lead to several novel applications. It has applications in various fields such as medical equipment, electronic devices, and energy storage [111–117]. Wang et al.

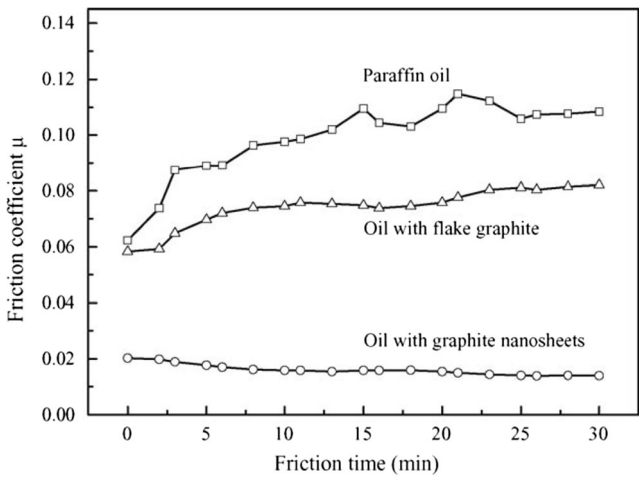

Fig. 24 Effect of graphite nanosheets on friction coefficient. Reprinted with permission from Ref. [105]

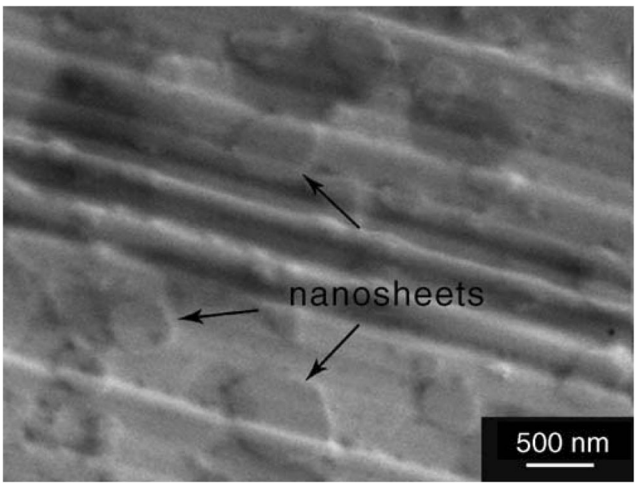

Fig. 25 Deposited graphitic nanosheets on the rubbing surface. Reprinted with permission from Ref. [105]

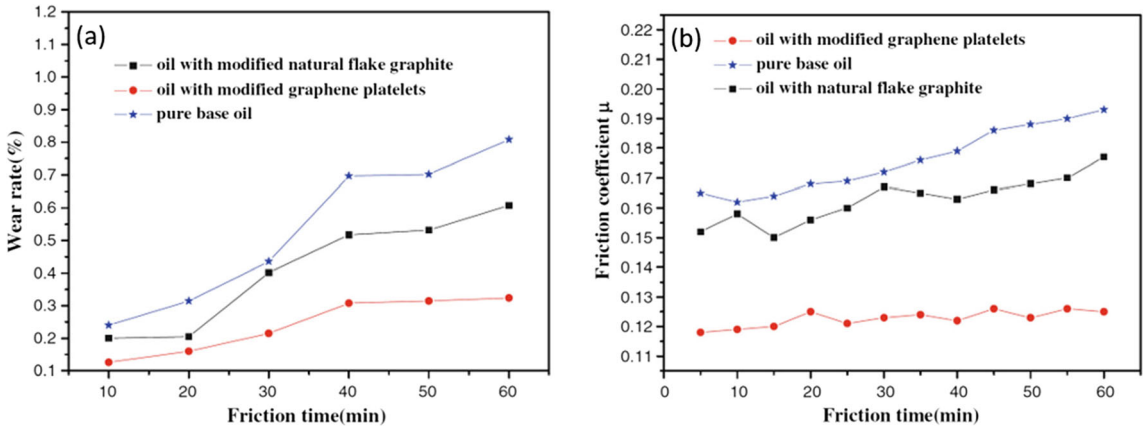

Fig. 26 **a** Wear rate and **b** friction coefficient variation with time for oil with modified natural flake graphite (0.075 wt.%) and oil with modified graphene platelets (0.075 wt.%) and pure base oil. Reprinted with permission from Ref. [104]

[111] demonstrated the use of graphene in dopamine detection. Dopamine is a well-known neurotransmitter, and it has been of interest due to its electrochemical activity. However, the coexistence of ascorbic acid that has similar oxidation potential makes it difficult to detect dopamine. In this work, the authors overcome the difficulty by modifying the electrode using graphene. They observed the unique phenomena that the positively charged dopamine was more sensitive than the negatively charged ascorbic acid toward the graphene-modified electrode. In comparison with multiwall carbon nanotubes modified electrode, the graphene-modified electrode detected the dopamine by eliminating the ascorbic acid. This unique electronic character of graphene can lead to the various applications in electrochemistry.

The superior conductivity of graphene leads to the application as an electrode material in electrical and optical devices. Apart from the electrical conductivity, graphene provides high optical transparency and excellent mechanical properties. Graphene grown on Cu by CVD process is reported to be the best material for electrode application because it has a minimum sheet resistance (300–350 Ω/□) and maximum transmittance (~ 90%) [112]. "Ω/□" is the unit for sheet resistance. The conductivity is further improved by doping and surface modification of graphene electrodes and can be used in various electronic, optical devices, such as molecular electronic devices, liquid crystal display, solar cells, and transparent and flexible devices [113]. Thus, graphene is a potential

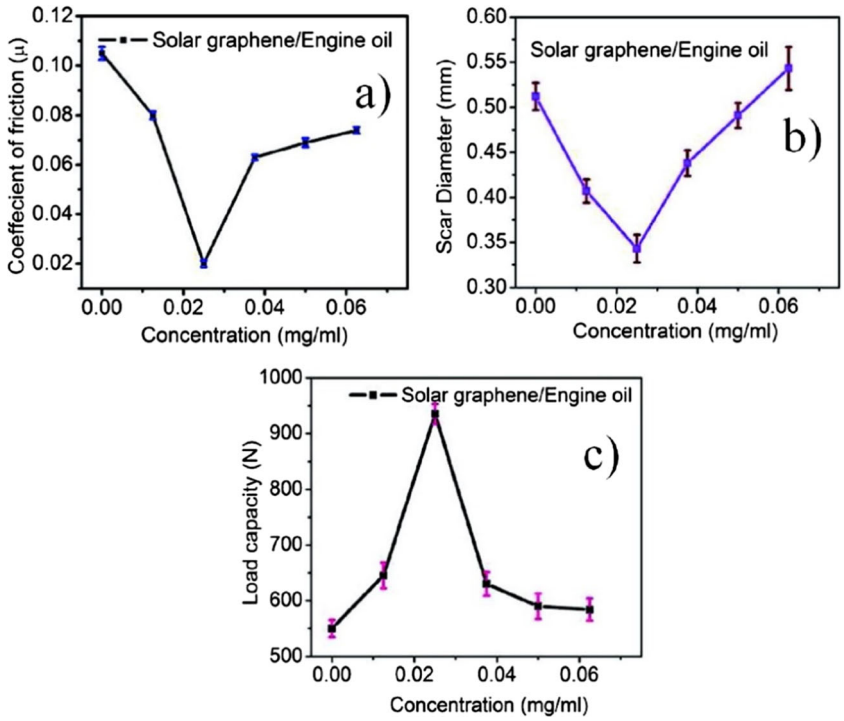

Fig. 27 Tribological properties variation with graphene content in engine oil **a** coefficient of friction, **b** wear scar diameter, and **c** load capacity. Reprinted with permission from Ref. [56]

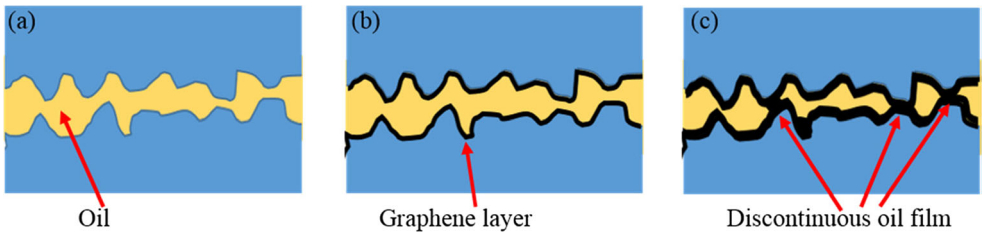

Fig. 28 Schematic for lubrication mechanism. **a** Pure oil, **b** oil with optimized graphene, and **c** oil with excess graphene as an additive

candidate to replace the traditional indium tin oxide electrodes.

In the field of energy storage, graphene can be used in the form of composites [114, 115]. Ding et al. [114] enhanced the conductivity of electrode for lithium iron phosphate ($LiFePO_4$) battery by addition of graphene in $LiFePO_4$. The nanostructured composite of $LiFePO_4$ and graphene was manufactured by co-precipitation method, and the resultant deposits were sintered followed by cooling and grinding. For electrochemical testing, Li metal was used as the anode. The composite material (1.5 wt.% graphene) showed drastically improvement in the capacity of the battery as shown in the voltage profile (Fig. 29). The $LiFePO_4$/graphene composites and $LiFePO_4$ showed the specific capacity of 160 and 113 mAh/g, respectively. The graphene nanosheets have been reported as conducting pathways between $LiFePO_4$ nanoparticles which overcome the limited conductivity issue of $LiFePO_4$ material.

Graphene also has the potential for corrosion resistance. Graphene coatings on metals, such as Ni and Cu, have been studied [116, 117]. Kirkland et al. [116] observed reduction in anodic and cathodic reaction rates by graphene coating on Ni. In the case of Cu, they found that graphene coating primarily inhibited the cathodic reaction. Though graphene is affecting the metals differently, it is providing a barrier to metal dissolution from the metal substrate. Thus, it can be a useful corrosion-resistant material.

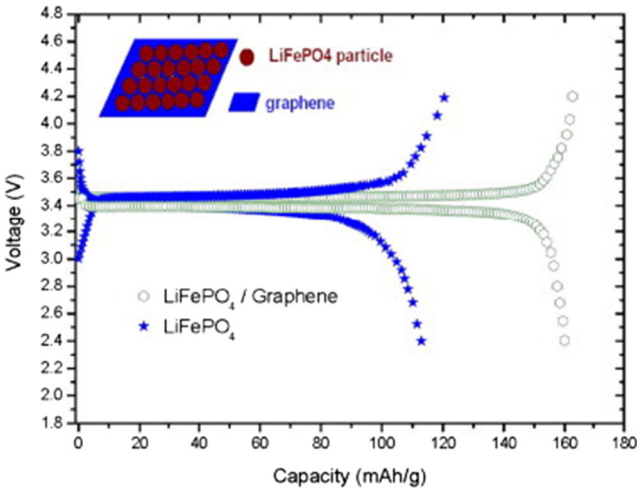

Fig. 29 Variation of voltage with the specific capacity for the $LiFePO_4$ and $LiFePO_4$/graphene composites. Reprinted with permission from Ref. [114]

Such extraordinary properties of graphene coupled with tribological properties can make it possible to design multifunctional composite for applications such as rotating electrical connector and bearing in the corrosive environment.

5 Conclusions

This review presents the current knowledge of excellent tribological properties of graphene, and it is clear that graphene has a strong potential to be used as reinforcement in the polymer, metal, and ceramic-matrix. As it is evident that graphene is a new material and the studies on graphene nanocomposites are in its early stages. Its self-lubricating tribological properties have not been explored much. For graphene/polymer nanocomposites, chemical interaction between polymer and graphene has to be studied vigorously because properties have been found to be dependent on polymers as well. The other critical problem is the uniform dispersion of graphene in the polymer that has been solved by functionalization/modification of graphene. However, the effect of functionalization/modification of graphene on the tribological properties of polymer composite materials have not been studied. For metal- and ceramic-matrix composites, it is important to understand the relevant wear mechanisms. The frictional properties of single-layer graphene have been found to be dependent on the substrate such as mica and Si due to adhesion. This provides a prospect of understanding adhesion phenomenon between graphene and metal or ceramic-matrix. Thus, the understanding of graphene interaction with different metals and ceramics can results in promising tribological properties.

The other important challenge is the development of stable transfer layer of graphene from bulk composite to the surface. It requires the systematic study of stress transfer during wear test by changing the tribological test parameters (load, velocity), surface properties (roughness and texture), and material properties (graphene content and matrix material). This study can predict the controlling parameters to supply graphene to the interface that can lead to better lubrication. It has also found that multilayered graphene has been beneficial and as it is known that in the case of graphite, low friction occurs by sliding of layers due to weak van der Waal force between graphitic layers. The same mechanism can apply to multilayered graphene structures, and knowledge of dependency on number of graphene layers can be a determining factor to

control wear properties of composites material. Properties and number of graphene layers are highly depends on the synthesis techniques. As it has been seen that mechanically exfoliated graphene layers have better tribological properties than the CVD and graphene oxide reduced graphene. Other properties for multifunctional nanocomposites such as size, chemical reactivity, and thermal conductivity can be controlled by selecting the proper synthesis technique. The most common method for laboratory purposes is the Hummers' method (chemical method) to produce graphene oxide followed by thermal annealing at higher temperature (~ 1000 °C) to reduce graphene oxide into graphene. For electrical and sensor applications, the most preferable methods are the thermal and plasma enhanced chemical vapor deposition directly on the substrates such as SiO_2 and Cu.

For graphene as an additive in the lubricant oil, it has seen that the formation of a protective layer of graphene provides superior lubrication than the pure oil. The optimized concentration of graphene has been observed to vary according to the lubricant oil, type of graphene, and test parameters such as load and rotating speed. However, none of the studies reported the relation between test parameters and deposition of graphene nanoplatelets or graphene oxide on the worn surface. A systematic study is required to understand the lubrication mechanism fully and to optimize the graphene content in the oil.

References

1. Lee C, Wei X, Kysar JW, Hone J (2008) Measurement of the elastic properties and intrinsic strength of monolayer graphene. Science 321(5887):385–388
2. Wu Z-S, Ren W, Gao L, Liu B, Jiang C, Cheng H-M (2009) Synthesis of high-quality graphene with a pre-determined number of layers. Carbon 47(2):493–499. https://doi.org/10.1016/j.carbon.2008.10.031
3. Ghosh S, Calizo I, Teweldebrhan D, Pokatilov EP, Nika DL, Balandin AA, Bao W, Miao F, Lau CN (2008) Extremely high thermal conductivity of graphene: prospects for thermal management applications in nanoelectronic circuits. Appl Phys Lett 92(15):151911
4. Raichura A, Dutta M, Stroscio MA (2004) Continuum model for acoustic phonons in nanotubes: phonon bottleneck. physica status solidi (b) 241 (15):3448-3453
5. Copper Annealed, MatWeb Materials Property Data (2017) http://www.matweb.com/search/datasheet.aspx?matguid=9aebe83845c04c1db5126fada6f76f7e. Accessed 26-06 2017
6. ASTM A36 Steel, MatWeb Materials Property Data. (2017) http://www.matweb.com/search/DataSheet.aspx?MatGUID=afc003f4fb40465fa3df05129f0e88e6&ckck=1. Accessed 26–06 2017
7. Compare ASTM A27 cast steel to ASTM A36 carbon steel. (2017) http://www.makeitfrom.com/compare/ASTM-A27-Cast-Carbon-Steel/ASTM-A36-SS400-S275-Structural-Carbon-Steel. Accessed 26–06 2017
8. Berman D, Deshmukh SA, Sankaranarayanan SKRS, Erdemir A, Sumant AV (2014) Extraordinary macroscale wear resistance of one atom thick graphene layer. Adv Funct Mater 24(42):6640–6646
9. Khun NW, Zhang H, Lim LH, Yang J (2015) Mechanical and tribological properties of graphene modified epoxy composites. KMUTNB Int J Appl Sci Technol 8(2):101–109
10. Xu Z, Shi X, Zhai W, Yao J, Song S, Zhang Q (2014) Preparation and tribological properties of TiAl matrix composites reinforced by multilayer graphene. Carbon 67:168–177
11. Pfeifer J, Sáfrán G, Wéber F, Zsigmond V, Koszor O, Arató P, Balázsi C Tribology study of silicon nitride-based nanocomposites with carbon additions. In, 2010. Trans Tech Publ, pp 235–238
12. Peng Y, Wang Z, Zou K (2015) Friction and wear properties of different types of graphene nanosheets as effective solid lubricants. Langmuir 31(28):7782–7791. https://doi.org/10.1021/acs.langmuir.5b00422
13. Viculis LM, Mack JJ, Kaner RB (2003) A chemical route to carbon nanoscrolls. Science 299(5611):1361–1361
14. Novoselov KS, Geim AK, Morozov SV, Jiang D, Zhang Y, Dubonos SV, Grigorieva IV, Firsov AA (2004) Electric field effect in atomically thin carbon films. Science 306(5696):666–669
15. Gass MH, Bangert U, Bleloch AL, Wang P, Nair RR, Geim AK (2008) Free-standing graphene at atomic resolution. Nat Nanotechnol 3(11):676–681
16. Meyer JC, Girit CO, Crommie MF, Zettl A (2008) Hydrocarbon lithography on graphene membranes. Appl Phys Lett 92(12):123110
17. Novoselov KS, Geim AK, Morozov SV, Dubonos SV, Zhang Y, Jiang D (2004) Room-temperature electric field effect and carrier-type inversion in graphene films. arXiv preprint cond-mat/0410631
18. Huc V, Bendiab N, Rosman N, Ebbesen T, Delacour C, Bouchiat V (2008) Large and flat graphene flakes produced by epoxy bonding and reverse exfoliation of highly oriented pyrolytic graphite. Nanotechnology 19(45):455601
19. Shukla A, Kumar R, Mazher J, Balan A (2009) Graphene made easy: high quality, large-area samples. Solid State Commun 149(17):718–721
20. Zhao W, Fang M, Wu F, Wu H, Wang L, Chen G (2010) Preparation of graphene by exfoliation of graphite using wet ball milling. J Mater Chem 20(28):5817–5819
21. Liu C, Hu G, Gao H (2012) Preparation of few-layer and single-layer graphene by exfoliation of expandable graphite in supercritical N, N-dimethylformamide. J Supercrit Fluids 63:99–104
22. Liu N, Luo F, Wu H, Liu Y, Zhang C, Chen J (2008) One-step ionic-liquid-assisted electrochemical synthesis of ionic-liquid-functionalized graphene sheets directly from graphite. Adv Funct Mater 18(10):1518–1525
23. Wang J, Manga KK, Bao Q, Loh KP (2011) High-yield synthesis of few-layer graphene flakes through electrochemical expansion of graphite in propylene carbonate electrolyte. J Am Chem Soc 133(23):8888–8891
24. Su C-Y, Lu A-Y, Xu Y, Chen F-R, Khlobystov AN, Li L-J (2011) High-quality thin graphene films from fast electrochemical exfoliation. ACS Nano 5(3):2332–2339
25. Somani PR, Somani SP, Umeno M (2006) Planer nano-graphenes from camphor by CVD. Chem Phys Lett 430(1–3):56–59. https://doi.org/10.1016/j.cplett.2006.06.081
26. Obraztsov AN, Obraztsova EA, Tyurnina AV, Zolotukhin AA (2007) Chemical vapor deposition of thin graphite films of nanometer thickness. Carbon 45(10):2017–2021. https://doi.org/10.1016/j.carbon.2007.05.028

27. Yu Q, Lian J, Siriponglert S, Li H, Chen YP, Pei S-S (2008) Graphene segregated on Ni surfaces and transferred to insulators. Appl Phys Lett 93(11):113103
28. De Arco LG, Zhang Y, Kumar A, Zhou C (2009) Synthesis, transfer, and devices of single-and few-layer graphene by chemical vapor deposition. IEEE Trans Nanotechnol 8(2):135–138
29. Zhang Y, Gomez L, Ishikawa FN, Madaria A, Ryu K, Wang C, Badmaev A, Zhou C (2010) Comparison of graphene growth on single-crystalline and polycrystalline Ni by chemical vapor deposition. J Phys Chem Lett 1(20):3101–3107
30. Wang JJ, Zhu MY, Outlaw RA, Zhao X, Manos DM, Holloway BC, Mammana VP (2004) Free-standing subnanometer graphite sheets. Appl Phys Lett 85(7):1265–1267
31. Wang J, Zhu M, Outlaw RA, Zhao X, Manos DM, Holloway BC (2004) Synthesis of carbon nanosheets by inductively coupled radio-frequency plasma enhanced chemical vapor deposition. Carbon 42(14):2867–2872. https://doi.org/10.1016/j.carbon.2004.06.035
32. Shang NG, Papakonstantinou P, McMullan M, Chu M, Stamboulis A, Potenza A, Dhesi SS, Marchetto H (2008) Catalyst-free efficient growth, orientation and biosensing properties of multilayer graphene nanoflake films with sharp edge planes. Adv Funct Mater 18(21):3506–3514
33. Kim YS, Lee JH, Kim YD, Jerng S-K, Joo K, Kim E, Jung J, Yoon E, Park YD, Seo S, Chun S-H (2013) Methane as an effective hydrogen source for single-layer graphene synthesis on Cu foil by plasma enhanced chemical vapor deposition. Nano 5(3):1221–1226. https://doi.org/10.1039/C2NR33034B
34. Terasawa T-o, Koichiro S (2012) Synthesis of nitrogen-doped graphene by plasma-enhanced chemical vapor deposition. Jpn J Appl Phys 51(5R):055101
35. Cheng L, Yun K, Lucero A, Huang J, Meng X, Lian G, Nam H-S, Wallace RM, Kim M, Venugopal A (2015) Low temperature synthesis of graphite on Ni films using inductively coupled plasma enhanced CVD. J Mater Chem C 3(20):5192–5198
36. Woo Y, Kim D-C, Jeon D-Y, Chung H-J, Shin S-M, Li X-S, Kwon Y-N, Seo DH, Shin J, Chung UI (2009) Large-grained and highly-ordered graphene synthesized by radio frequency plasma-enhanced chemical vapor deposition. ECS Trans 19(5):111–114
37. Wang SM, Pei YH, Wang X, Wang H, Meng QN, Tian HW, Zheng XL, Zheng WT, Liu YC (2010) Synthesis of graphene on a polycrystalline Co film by radio-frequency plasma-enhanced chemical vapour deposition. J Phys D Appl Phys 43(45):455402
38. Rollings E, Gweon GH, Zhou SY, Mun BS, McChesney JL, Hussain BS, Fedorov AV, First PN, de Heer WA, Lanzara A (2006) Synthesis and characterization of atomically thin graphite films on a silicon carbide substrate. J Phys Chem Solids 67(9–10):2172–2177. https://doi.org/10.1016/j.jpcs.2006.05.010
39. Berger C, Song Z, Li T, Li X, Ogbazghi AY, Feng R, Dai Z, Marchenkov AN, Conrad EH, First PN (2004) Ultrathin epitaxial graphite: 2D electron gas properties and a route toward graphene-based nanoelectronics. J Phys Chem B 108(52):19912–19916
40. Hass J, De Heer WA, Conrad EH (2008) The growth and morphology of epitaxial multilayer graphene. J Phys Condens Matter 20(32):323202
41. Ohta T, El Gabaly F, Bostwick A, McChesney JL, Emtsev KV, Schmid AK, Seyller T, Horn K, Rotenberg E (2008) Morphology of graphene thin film growth on SiC (0001). New J Phys 10(2):023034
42. Hummers WS Jr, Offeman RE (1958) Preparation of graphitic oxide. J Am Chem Soc 80(6):1339–1339
43. Sahu SR, Devi MM, Mukherjee P, Sen P, Biswas K (2013) Optical property characterization of novel graphene-X (X = Ag, Au and Cu) nanoparticle hybrids. J Nanomater 2013:6
44. Marcano DC, Kosynkin DV, Berlin JM, Sinitskii A, Sun Z, Slesarev A, Alemany LB, Lu W, Tour JM (2010) Improved synthesis of graphene oxide. ACS Nano 4(8):4806–4814
45. Wang F, Zhang K (2011) Reduced graphene oxide–TiO 2 nanocomposite with high photocatalystic activity for the degradation of rhodamine B. J Mol Catal A Chem 345(1):101–107
46. Xu Y, Sheng K, Li C, Shi G (2011) Highly conductive chemically converted graphene prepared from mildly oxidized graphene oxide. J Mater Chem 21(20):7376–7380
47. Tan LL, Chai SP, Mohamed AR (2012) Synthesis and applications of graphene-based TiO2 photocatalysts. ChemSusChem 5(10):1868–1882
48. Liu H, Li Y, Wang T, Wang Q (2012) In situ synthesis and thermal, tribological properties of thermosetting polyimide/graphene oxide nanocomposites. J Mater Sci 47(4):1867–1874. https://doi.org/10.1007/s10853-011-5975-9
49. Juang Z-Y, Wu C-Y, Lo C-W, Chen W-Y, Huang C-F, Hwang J-C, Chen F-R, Leou K-C, Tsai C-H (2009) Synthesis of graphene on silicon carbide substrates at low temperature. Carbon 47(8):2026–2031. https://doi.org/10.1016/j.carbon.2009.03.051
50. Garaj S, Hubbard W, Golovchenko JA (2010) Graphene synthesis by ion implantation. Appl Phys Lett 97(18):183103
51. De Parga ALV, Calleja F, Borca B, Passeggi MCG Jr, Hinarejos JJ, Guinea F, Miranda R (2008) Periodically rippled graphene: growth and spatially resolved electronic structure. Phys Rev Lett 100(5):056807
52. Cano-Márquez AG, Rodríguez-Macías FJ, Campos-Delgado J, Espinosa-González CG, Tristán-López F, Ramírez-González D, Cullen DA, Smith DJ, Terrones M, Vega-Cantú YI (2009) Ex-MWNTs: graphene sheets and ribbons produced by lithium intercalation and exfoliation of carbon nanotubes. Nano Lett 9(4):1527–1533
53. Jiao L, Zhang L, Wang X, Diankov G, Dai H (2009) Narrow graphene nanoribbons from carbon nanotubes. Nature 458(7240):877–880
54. Kosynkin DV, Higginbotham AL, Sinitskii A, Lomeda JR, Dimiev A, Price BK, Tour JM (2009) Longitudinal unzipping of carbon nanotubes to form graphene nanoribbons. Nature 458(7240):872–876
55. Kim C-D, Min B-K, Jung W-S (2009) Preparation of graphene sheets by the reduction of carbon monoxide. Carbon 47(6):1610–1612
56. Eswaraiah V, Sankaranarayanan V, Ramaprabhu S (2011) Graphene-based engine oil nanofluids for tribological applications. ACS Appl Mater Interfaces 3(11):4221–4227
57. Jeon I-Y, Choi H-J, Jung S-M, Seo J-M, Kim M-J, Dai L, Baek J-B (2012) Large-scale production of edge-selectively functionalized graphene nanoplatelets via ball milling and their use as metal-free electrocatalysts for oxygen reduction reaction. J Am Chem Soc 135(4):1386–1393
58. Liu J, Poh CK, Zhan D, Lai L, Lim SH, Wang L, Liu X, Gopal Sahoo N, Li C, Shen Z, Lin J (2013) Improved synthesis of graphene flakes from the multiple electrochemical exfoliation of graphite rod. Nano Energy 2(3):377–386. https://doi.org/10.1016/j.nanoen.2012.11.003
59. Lee C, Wei X, Li Q, Carpick R, Kysar JW, Hone J (2009) Elastic and frictional properties of graphene. physica status solidi (b) 246(11-12):2562-2567
60. Filleter T, Bennewitz R (2010) Structural and frictional properties of graphene films on SiC (0001) studied by atomic force microscopy. Phys Rev B 81(15):155412
61. Choi JS, Kim J-S, Byun I-S, Lee DH, Lee MJ, Park BH, Lee C, Yoon D, Cheong H, Lee KH (2011) Friction anisotropy-driven domain imaging on exfoliated monolayer graphene. Science 333(6042):607–610

62. Choi JS, Kim J-S, Byun I-S, Lee DH, Hwang IR, Park BH, Choi T, Park JY, Salmeron M (2012) Facile characterization of ripple domains on exfoliated graphene. Rev Sci Instrum 83(7):073905
63. Li Q, Lee C, Carpick RW, Hone J (2010) Substrate effect on thickness-dependent friction on graphene. physica status solidi (b) 247 (11-12):2909-2914
64. Miracle DB (2005) Metal matrix composites—from science to technological significance. Compos Sci Technol 65(15):2526–2540
65. Fusaro RL (1990) Self-lubricating polymer composites and polymer transfer film lubrication for space applications. Tribol Int 23(2):105–122. https://doi.org/10.1016/0301-679X(90)90043-O
66. Voevodin AA, Zabinski JS (2005) Nanocomposite and nanostructured tribological materials for space applications. Compos Sci Technol 65(5):741–748. https://doi.org/10.1016/j.compscitech.2004.10.008
67. Raj R, Maroo SC, Wang EN (2013) Wettability of graphene. Nano Lett 13(4):1509–1515
68. Li Y, Wang Q, Wang T, Pan G (2012) Preparation and tribological properties of graphene oxide/nitrile rubber nanocomposites. J Mater Sci 47(2):730–738
69. Tai Z, Chen Y, An Y, Yan X, Xue Q (2012) Tribological behavior of UHMWPE reinforced with graphene oxide nanosheets. Tribol Lett 46(1):55–63. https://doi.org/10.1007/s11249-012-9919-6
70. Ionita M, Pandele AM, Crica L, Pilan L (2014) Improving the thermal and mechanical properties of polysulfone by incorporation of graphene oxide. Compos Part B 59:133–139
71. Wang H, Xie G, Fang M, Ying Z, Tong Y, Zeng Y (2017) Mechanical reinforcement of graphene/poly(vinyl chloride) composites prepared by combining the in-situ suspension polymerization and melt-mixing methods. Compos Part B 113:278–284. https://doi.org/10.1016/j.compositesb.2017.01.053
72. Tang Z, Lei Y, Guo B, Zhang L, Jia D (2012) The use of rhodamine B-decorated graphene as a reinforcement in polyvinyl alcohol composites. Polymer 53(2):673–680
73. Li Y, Wang S, Wang Q (2017) Enhancement of tribological properties of polymer composites reinforced by functionalized graphene. Compos Part B 120:83–91. https://doi.org/10.1016/j.compositesb.2017.03.063
74. Ren G, Zhang Z, Zhu X, Ge B, Guo F, Men X, Liu W (2013) Influence of functional graphene as filler on the tribological behaviors of Nomex fabric/phenolic composite. Composites Part A: Applied Science and Manufacturing 49 (Supplement C):157-164. doi: https://doi.org/10.1016/j.compositesa.2013.03.001
75. Wang Z, Nelson JK, Miao J, Linhardt RJ, Schadler LS, Hillborg H, Zhao S (2012) Effect of high aspect ratio filler on dielectric properties of polymer composites: a study on barium titanate fibers and graphene platelets. IEEE Trans Dielectr Electr Insul 19(3):960–967
76. Potts JR, Dreyer DR, Bielawski CW, Ruoff RS (2011) Graphene-based polymer nanocomposites. Polymer 52(1):5–25
77. Shiu S-C, Tsai J-L (2014) Characterizing thermal and mechanical properties of graphene/epoxy nanocomposites. Compos Part B 56:691–697
78. Moghadam AD, Omrani E, Menezes PL, Rohatgi PK (2015) Mechanical and tribological properties of self-lubricating metal matrix nanocomposites reinforced by carbon nanotubes (CNTs) and graphene–a review. Compos Part B 77:402–420
79. Hu Z, Tong G, Nian Q, Xu R, Saei M, Chen F, Chen C, Zhang M, Guo H, Xu J (2016) Laser sintered single layer graphene oxide reinforced titanium matrix nanocomposites. Compos Part B 93:352–359. https://doi.org/10.1016/j.compositesb.2016.03.043
80. Moghadam AD, Schultz BF, Ferguson JB, Omrani E, Rohatgi PK, Gupta N (2014) Functional metal matrix composites: self-lubricating, self-healing, and nanocomposites-an outlook. JOM 66(6):872–881
81. Wang J, Li Z, Fan G, Pan H, Chen Z, Zhang D (2012) Reinforcement with graphene nanosheets in aluminum matrix composites. Scr Mater 66(8):594–597
82. Ghazaly A, Seif B, Salem HG (2013) Mechanical and tribological properties of AA2124-graphene self lubricating nanocomposite. Light Metals 2013:411–415
83. Kuzumaki T, Miyazawa K, Ichinose H, Ito K (1998) Processing of carbon nanotube reinforced aluminum composite. J Mater Res 13(09):2445–2449
84. Kwon H, Park DH, Silvain JF, Kawasaki A (2010) Investigation of carbon nanotube reinforced aluminum matrix composite materials. Compos Sci Technol 70(3):546–550
85. Wozniak J, Kostecki M, Cygan T, Buczek M, Olszyna A (2017) Self-lubricating aluminium matrix composites reinforced with 2D crystals. Compos Part B 111:1–9. doi: https://doi.org/10.1016/j.compositesb.2016.11.054
86. Tabandeh-Khorshid M, Omrani E, Menezes PL, Rohatgi PK (2016) Tribological performance of self-lubricating aluminum matrix nanocomposites: role of graphene nanoplatelets. Eng Sci Technol Int J 19(1):463–469. https://doi.org/10.1016/j.jestch.2015.09.005
87. Rengifo S, Zhang C, Harimkar S, Boesl B, Agarwal A (2017) Tribological behavior of spark plasma sintered aluminum-graphene composites at room and elevated temperatures. Technologies 5(1):4
88. Chmielewski M, Michalczewski R, Piekoszewski W, Kalbarczyk M (2016) Tribological behaviour of copper-graphene composite materials. Key Eng Mater 674
89. Hu Z, Chen F, Xu J, Ma Z, Guo H, Chen C, Nian Q, Wang X, Zhang M (2017) Fabricating graphene-titanium composites by laser sintering PVA bonding graphene titanium coating: microstructure and mechanical properties. Compos Part B. https://doi.org/10.1016/j.compositesb.2017.09.069
90. Porwal H, Tatarko P, Saggar R, Grasso S, Kumar Mani M, Dlouhý I, Dusza J, Reece MJ (2014) Tribological properties of silica–graphene nano-platelet composites. Ceramics International 40 (8, Part A):12067-12074. doi: https://doi.org/10.1016/j.ceramint.2014.04.046
91. Belmonte M, Ramírez C, González-Julián J, Schneider J, Miranzo P, Osendi MI (2013) The beneficial effect of graphene nanofillers on the tribological performance of ceramics. Carbon 61:431–435. https://doi.org/10.1016/j.carbon.2013.04.102
92. Hvizdoš P, Dusza J, Balázsi C (2013) Tribological properties of Si3N4–graphene nanocomposites. J Eur Ceram Soc 33(12):2359–2364. https://doi.org/10.1016/j.jeurceramsoc.2013.03.035
93. Balko J, Hvizdoš P, Dusza J, Balázsi C, Gamcová J (2014) Wear damage of Si3N4-graphene nanocomposites at room and elevated temperatures. J Eur Ceram Soc 34(14):3309–3317. https://doi.org/10.1016/j.jeurceramsoc.2014.02.025
94. Gutierrez-Gonzalez CF, Smirnov A, Centeno A, Fernández A, Alonso B, Rocha VG, Torrecillas R, Zurutuza A, Bartolome JF (2015) Wear behavior of graphene/alumina composite. Ceram Int 41(6):7434–7438. https://doi.org/10.1016/j.ceramint.2015.02.061
95. Zhang C, Nieto A, Agarwal A (2016) Ultrathin graphene tribofilm formation during wear of Al2O3–graphene composites. Nanomater Energy 5(1):1–9
96. Zhu Q, Shi X, Zhai W, Yao J, Ibrahim AMM, Xu Z, Song S, ud Din AQ, Chen L, Xiao Y (2014) Effect of counterface balls on the friction layer of Ni3Al matrix composites with 1.5 wt% graphene nanoplatelets. Tribol Lett 55 (2):343–352
97. Porwal H, Grasso S, Reece MJ (2013) Review of graphene–ceramic matrix composites. Adv Appl Ceram 112(8):443–454
98. Walker LS, Marotto VR, Rafiee MA, Koratkar N, Corral EL (2011) Toughening in graphene ceramic composites. ACS Nano 5(4):3182–3190

99. Wang K, Wang Y, Fan Z, Yan J, Wei T (2011) Preparation of graphene nanosheet/alumina composites by spark plasma sintering. Mater Res Bull 46(2):315–318. https://doi.org/10.1016/j.materresbull.2010.11.005
100. Ramirez C, Figueiredo FM, Miranzo P, Poza P, Osendi MI (2012) Graphene nanoplatelet/silicon nitride composites with high electrical conductivity. Carbon 50(10):3607–3615
101. Fan Y, Jiang W, Kawasaki A (2012) Highly conductive few-layer graphene/Al2O3 nanocomposites with tunable charge carrier type. Adv Funct Mater 22(18):3882–3889
102. Fang M, Wang K, Lu H, Yang Y, Nutt S (2009) Covalent polymer functionalization of graphene nanosheets and mechanical properties of composites. J Mater Chem 19(38):7098–7105
103. Stankovich S, Dikin DA, Dommett GHB, Kohlhaas KM, Zimney EJ, Stach EA, Piner RD, Nguyen ST, Ruoff RS (2006) Graphene-based composite materials. Nature 442 (7100):282-286
104. Lin J, Wang L, Chen G (2011) Modification of graphene platelets and their tribological properties as a lubricant additive. Tribol Lett 41(1):209–215
105. Huang HD, Tu JP, Gan LP, Li CZ (2006) An investigation on tribological properties of graphite nanosheets as oil additive. Wear 261(2):140–144. https://doi.org/10.1016/j.wear.2005.09.010
106. Lu K (2008) Theoretical analysis of colloidal interaction energy in nanoparticle suspensions. Ceram Int 34(6):1353–1360. https://doi.org/10.1016/j.ceramint.2007.02.016
107. Zhang W, Zhou M, Zhu H, Tian Y, Wang K, Wei J, Ji F, Li X, Li Z, Zhang P (2011) Tribological properties of oleic acid-modified graphene as lubricant oil additives. J Phys D Appl Phys 44(20): 205303
108. Senatore A, D'Agostino V, Petrone V, Ciambelli P, Sarno M (2013) Graphene oxide nanosheets as effective friction modifier for oil lubricant: materials, methods, and tribological results. ISRN Tribology 2013
109. Song H-J, Li N (2011) Frictional behavior of oxide graphene nanosheets as water-base lubricant additive. Applied Physics A 105(4):827–832
110. Kinoshita H, Nishina Y, Alias AA, Fujii M (2014) Tribological properties of monolayer graphene oxide sheets as water-based lubricant additives. Carbon 66:720–723. https://doi.org/10.1016/j.carbon.2013.08.045
111. Wang Y, Li Y, Tang L, Lu J, Li J (2009) Application of graphene-modified electrode for selective detection of dopamine. Electrochem Commun 11(4):889–892
112. Jo G, Choe M, Lee S, Park W, Kahng YH, Lee T (2012) The application of graphene as electrodes in electrical and optical devices. Nanotechnology 23(11):112001
113. Liang M, Luo B, Zhi L (2009) Application of graphene and graphene-based materials in clean energy-related devices. Int J Energy Res 33(13):1161–1170
114. Ding Y, Jiang Y, Xu F, Yin J, Ren H, Zhuo Q, Long Z, Zhang P (2010) Preparation of nano-structured LiFePO 4/graphene composites by co-precipitation method. Electrochem Commun 12(1): 10–13
115. Chang K, Chen W (2011) L-cysteine-assisted synthesis of layered MoS2/graphene composites with excellent electrochemical performances for lithium ion batteries. ACS Nano 5(6):4720–4728
116. Kirkland NT, Schiller T, Medhekar N, Birbilis N (2012) Exploring graphene as a corrosion protection barrier. Corros Sci 56:1–4
117. Prasai D, Tuberquia JC, Harl RR, Jennings GK, Bolotin KI (2012) Graphene: corrosion-inhibiting coating. ACS Nano 6(2):1102–1108